 doi:10.20944/preprints202011.0547.v1

Minireview

Carbon Dots as a sustainable new platform for organic light emitting diode

Paola Lagonegro,[1] Umberto Giovanella,[1]* and Mariacecilia Pasini[1]*

[1] Istituto di Scienze e Tecnologie Chimiche (SCITEC), Consiglio Nazionale delle Ricerche (CNR), via A. Corti 12, 20133 Milano (Italy)

* Correspondence: U.G. umberto.giovanella@scitec.cnr.it; M.P. mariacecilia.pasini@scitec.cnr.it

Abstract: In the last 10 years, carbon dots (CDs) synthesized from renewable organic resources have been gathered a considerable amount of attention in different fields for their peculiar photoluminescent properties. Moreover, the synthesis of CDs fully responds to the principles of the circular chemistry and the concept of safe-by-design. This review will focus on the different strategies for the incorporation of CDs in organic light-emitting devices (OLEDs) and on the study of the impact of CDs properties on the OLEDs performance. The main current research outcomes and highlights are summarized to guide users towards the fully exploitation of use these materials in optoelectronic applications.

Keywords: Carbon dots; organic light-emitting diode; photoluminescence

1. Introduction

The growing demand for electronic devices for an ever-increasing number of applications means that green and sustainable electronics are no longer just a dream, but a pressing need [1].

In this context the electronics and optoelectronics based on organic semiconductor showed, in the last few years, significant growth in many areas dominated by conventional electronics [2]. The foremost advantage of organic materials is that they are cheap, lightweight, easy to be processed and flexible [3]. However, the most effective synthetic methodologies [4] currently employed for producing organic semiconductors are affected by safety and environmental issues which may seriously prevent their large-scale production. In this regard, the application of principles of green chemistry for the development of waste-minimized and cleaner synthetic approaches to semiconductor synthesis is essential for propelling the field of organic electronics thus moving towards increasingly sustainable electronic devices [5].

In fact, the use of organic materials to build electronic devices [6] holds the promise that future electronic manufacturing methods will rely on safer and more abundant raw materials [7]. The vision is for resource-efficient synthetic methodologies, whereby both devices themselves and manufacturing of those devices use less and safe materials.

The first pillar on which the new sustainable industrial revolution is based is inevitably the development of new materials that are possibly safe and sustainable by design [8].

Among the emerging classes of materials able to meet these needs, carbon dots (CDs), member of nanocarbon family that comprise, differently from the best known carbon nanotube [9], discrete quasi-spherical nanoparticles with sizes below 10 nm, are being attracting considerable interest. Since their first discovery in 2006, CDs [10,11] have gained ever-increasing attention due to their fascinating properties like unique optical behaviour, tunable emission, multiple functional groups, excellent biocompatibility, chemical and photo-stability, low toxicity and low-cost. More importantly, their properties can be tailored by controlling the size, shape and heteroatom doping of CDs and by

Preprints (www.preprints.org) | NOT PEER-REVIEWED | Posted: 20 November 2020 doi:10.20944/preprints202011.0547.v1

modifying their surfaces and edges, due to the remarkable quantum confinement effect (QCE), surface effect and edge effect [12], (Fig.1). They are considered as promising green alternatives to fluorescent dyes [13–15] and generally to toxic metallic colloidal semiconductor nanocrystals, and are advocated for diversified applications such as sensing, bioimaging, fingerprint detection, gene delivery , solar cells, printing inks and optoelectronic applications in general [12,16–19] (Fig.1 and 2).

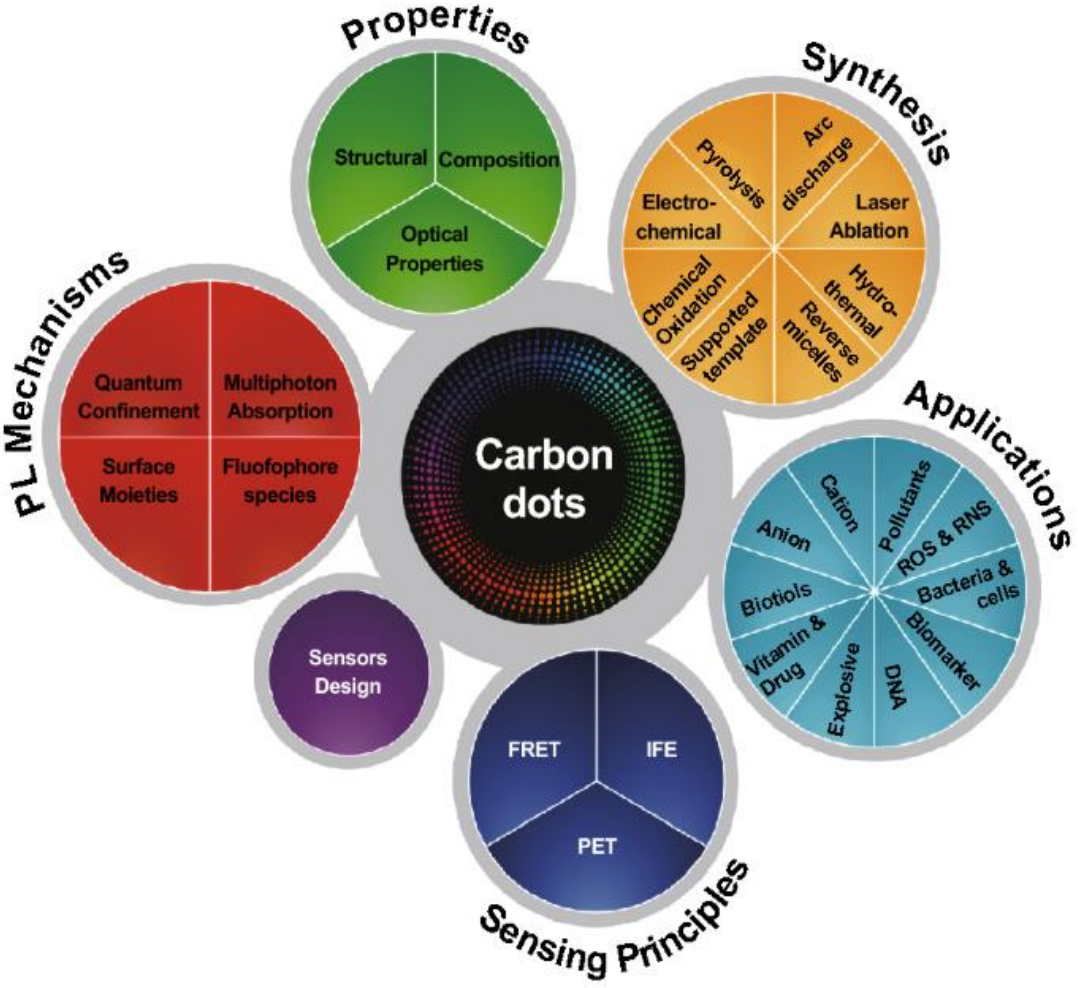

Figure 1. Carbon Dots General overview. Reprinted with permission from [19] Copyright 2019 Springer.

Preparation methods of CDs reported so far can broadly be grouped into top-down and bottom-up approaches. The top-down strategy [20–27] involves the breakdown of bulk carbon sources like graphite, carbon nanotubes, and nanodiamonds into fluorescent CDs by employing techniques like arc discharge, laser ablation, chemical oxidation in strong acid and electrochemical synthesis. Conversely, in the bottom-up approach [28–32, 33, 34] the CDs are formed from molecular precursors by applying solvothermal/hydrothermal methods, ultrasound/microwave treatments, or simple thermal combustion.

Although a large variety of techniques and starting materials were employed for the production of CDs, the demand for the sustainable synthetic routes, that adhere to the principles of green chemistry, is prominent. It has been demonstrated that CDs can be prepared in principle from any starting materials that contain carbon. This, in particular, guarantees that most by-products of the food supply chain can be reused to produce CDs. Agriculture products contain a myriad of natural molecules that can make up a diverse source of surface functional groups in CDs formation.

A relevant feature for CDs sustainability has to do with the synthetic methodologies for their fabrication. CDs can be produced hydrothermally, that is, by heating the starting materials in water under atmosphere or elevated pressure [28–31,34,35]. Consequently, the cost of production is low, and the operation is easy, relatively safe, and free of organic solvents. Furthermore, shorter

Preprints (www.preprints.org) | NOT PEER-REVIEWED | Posted: 20 November 2020 doi:10.20944/preprints202011.0547.v1

processing time and lower energy consumption for CD manufacture can be obtained when microwave is used as the heating source [36,37].

Toxicity studies of the CDs were performed with both plants and animals (mice) revealing good biocompatibility [38,39,40] and opened the way not only to their bio-applications, but also to a biodegradable electronics [19,40].

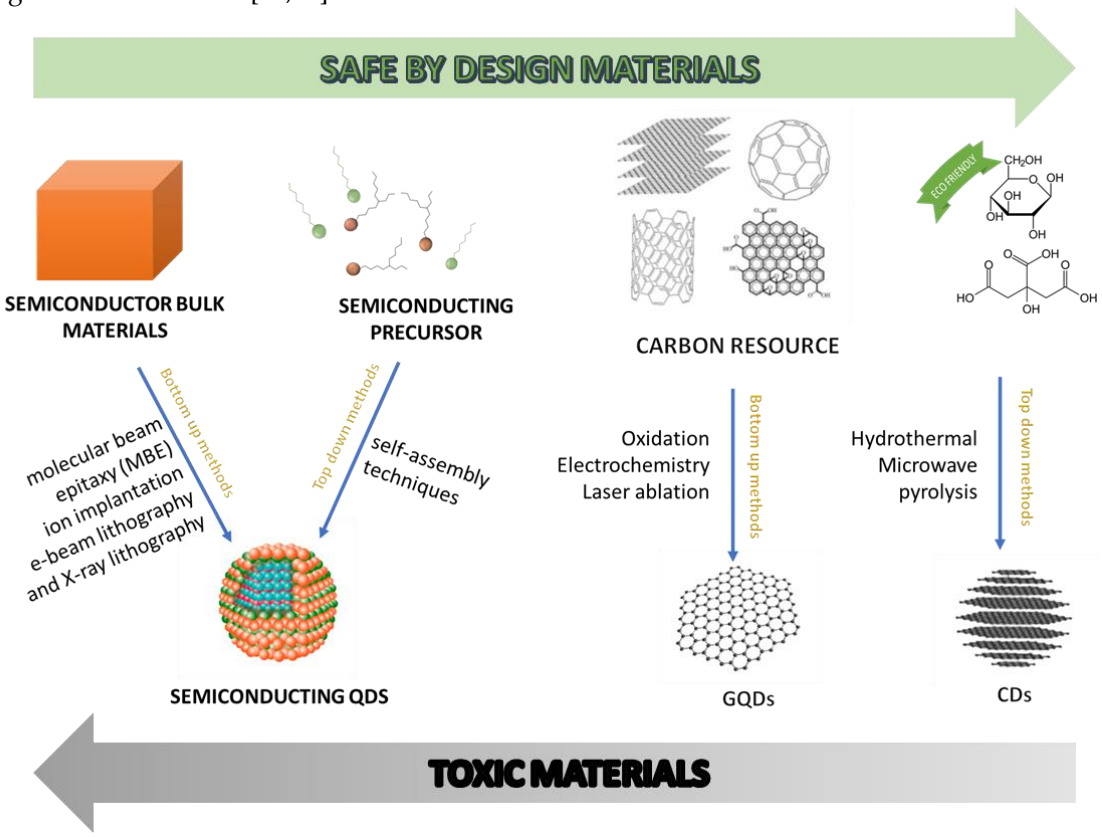

Figure 2. Schematic representation of Carbon Dots main characteristics. Adapted with permission from [14] Copyright 2019 American chemical society. Adapted with permission from [41] Copyright 2017 Elsevier.

With this perspective, in the present minireview we will discuss CDs obtained with a bottom up approach as it is the one that best adheres to the principles of green chemistry. They can in fact be obtained from renewable sources or waste [37], the synthesis methodologies are simple and inexpensive, and they do not require the use of metal catalysts or chlorinated solvents. We will focalized on CDs as a sustainable new platform for OLEDs [42,43] without deepening the methods of synthesis on which relevant works have already been written [28-37,44]. In Fact, among the various interesting applications of organic electronics, the OLEDs are certainly those that have already carved out a slice of the market [42] and for this reason the development of sustainable active materials and green technologies can already help the economy in a GREEN turn.

In the next Section 2, we will make a brief introduction on the type and optical properties of these luminescent carbon materials. Section 3 will cover their different application in electroluminescence devices as active layer or as charge regulating layer. In the last section, we will give perspectives for CDs including potential applications and possible development in particular as promising candidate for a safe-by-design material. We hope that this review will provide critical insights to inspire new exciting discoveries on CDs from both fundamental and practical standpoints so that the realization of their potential in the optoelectronic area can be facilitated.

2 Definition of Carbon dots and optical properties

 doi:10.20944/preprints202011.0547.v1

Since their fortuitous discovery in 2004 by Xu et al. [10] and subsequently by Sun et al. in 2006 [11], CDs attracted a great deal of attention. Generally, CDs are 0-dimension nanocarbons with a typical size of less than 10 nm, although ~60 nm size CDs have also been reported. CDs are quasispherical nanoparticles consisting of amorphous and crystalline parts, mainly composed of carbon. The height of CDs ranges from 0.5 to 5 nm depending on the preparation methods, with a crystal lattice with an interlayer difference of 0.34 nm, which corresponds to the (002) interlayer spacing of graphite [12-14]. CDs are often confused, or associated, with graphene quantum dots (GQDs) [15] which are always part of the family of carbon based nanomaterials, but have different characteristics and origins. In fact, GQDs are nanofragments of graphene, they have one or few layers of graphene and usually a larger horizontal dimension than in height with thickness of less than 2 nm exhibiting a typical fringe spacing of 0.24 nm associated with the (100) in-plane lattice spacing of graphene and they are generally produced from graphene or graphene oxide via top-down approaches [14].

Over the last 15 years, CDs have been synthesized with different approaches (i.e. top down and bottom up) however, only recently sustainable precursors and methodology have been deeply investigated for their production [45,46]. These approaches look for sustainable materials which are low-cost, scalable, industrially and economically attractive, and based on renewable and highly abundant resources. This means that CDs synthesis can meet the requirements of the circular chemistry. Interestingly, after preparation from solution, CDs can be functionalized with complex surface groups, especially oxygen based functional groups, such as carboxyl and hydroxyl, which impart excellent water solubility and suitable chemically reactive groups for surface passivation and derivatization with various organic materials. These surface groups make great contributions to the optical properties of CDs. For instance, upon surface passivation, the fluorescence properties of CDs can be enhanced.[47,48] Surface functionalization modifies the physical properties of CDs as their solubility in aqueous and non-aqueous solvents. In addition, the large conjugated structure endows CDs with some important characteristics, like good photostability, high surface area, and robust surface grafting [49]. Their electronic structures can be tuned by their size, shape, surface functional groups and heteroatom doping, as theoretical investigated and experimental confirmed by several groups [50–54]. The tunability of optoelectronic properties by modifying synthetic parameters and precursor strictly resembled the conjugated polymers features [55].

As mentioned above the CDs emission properties are their most amazing characteristics [41]. and significant advances have been made in the last years reaching photoluminescence quantum yield (PLQY) up to 80% in CDs produced from citric acid as renewable precursor, or bright and stable PLQY of 26% converting toxic cigarette butts[28, 54].

Mostly, CD are blue emitter, but emission from ultraviolet to near-infrared was reported [55, 56] as well as white light emission [59]. In general their PL spectra are symmetrical and broad with large Stokes shifts (mainly due to the CDs large size distribution) and the PL spectra usually have an excitation-dependent behaviour, with the emission peak varying with the excitation wavelength [22, 58].

The emission mechanism of CDs is a longstanding debate and several hypotheses have been proposed [41] (see Fig.3) such as i) size-dependent emission, ii) surface state-derived luminescence, and iii) embedded molecular luminophore [61]. Regardless of the type of mechanism, it has been shown that the CDs emission could be regulated by controlling their size (mainly referring to sp^2 carbon domains), heteroatom doping, and surface functionalization [60,61,62].

Preprints (www.preprints.org) | NOT PEER-REVIEWED | Posted: 20 November 2020 doi:10.20944/preprints202011.0547.v1

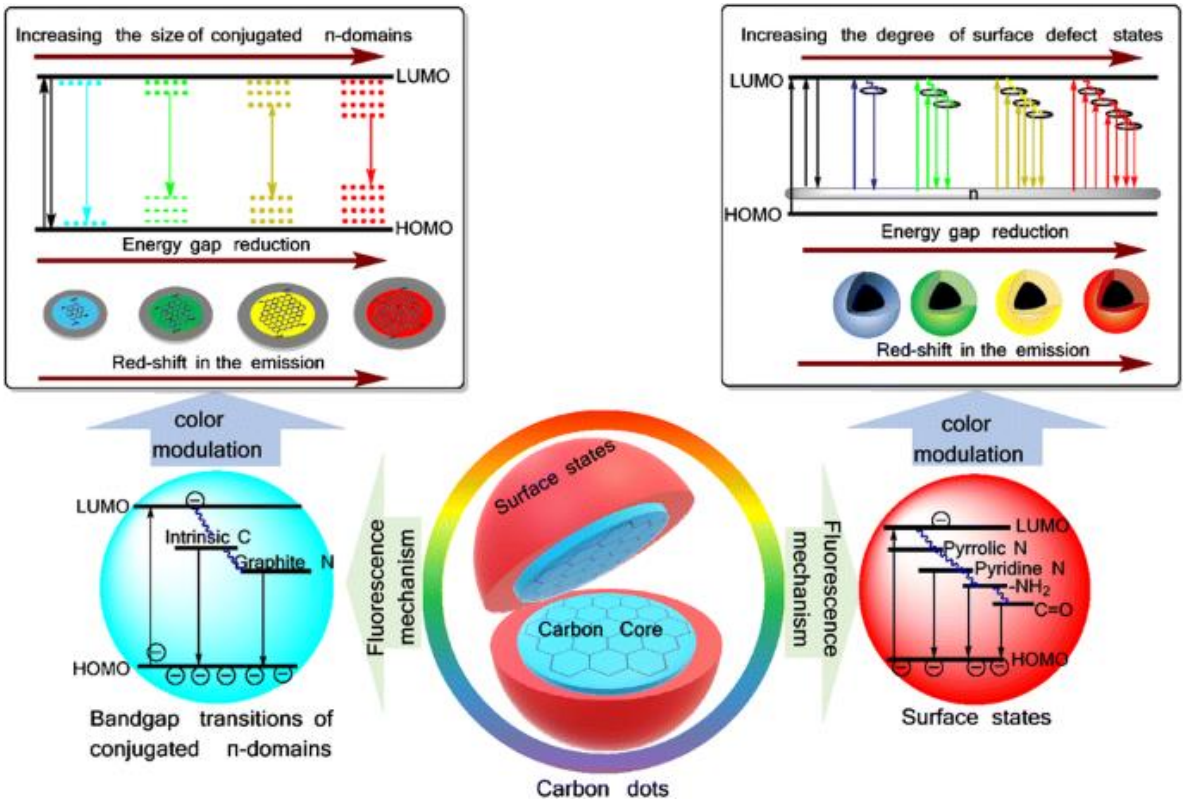

Figure 3. Different hypothesis for CDs emission mechanism. Reprinted with permission from [64] Copyright 2019 Springer Nature.

The first hypothesis proposed is based on the size of CDs [61]. Yuan and co-workers synthetized multicolour-emitting CDs with different dimensions from citric acid (CA) and diaminonaphthalene (DAN) by controlling the process parameter. CDs showed average sizes of about 1.95, 2.41, 3.78, 4.90 and 6.68 nm (Fig.4a), with a corresponding blue (430 nm), green (513 nm), yellow (535 nm), orange (565 nm), and red (565 nm) emission, respectively (Fig.4b). In according with results, they deduced that by increasing the size of CDs and consequently the conjugated π-domain, the bandgap decreases (fig.4c) [65].

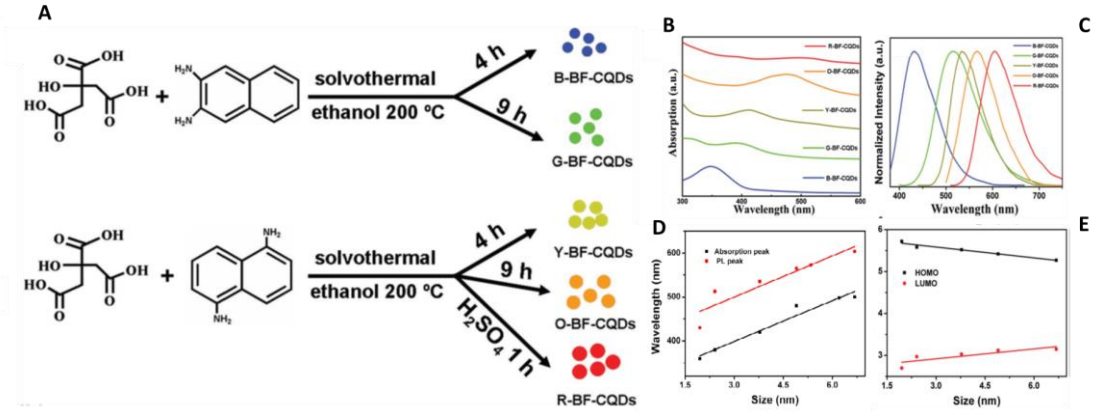

Figure 4. Preparation of bright multicolor bandgap fluorescent (BS) CDs from blue to red by solvothermal treatment of CA and DAN. Reprinted with permission from [63] Copyright 2016 WILEY-VCH Verlag GmbH & Co. KGaA, Weinheim

A second hypothesis is related to the surface states of CDs. Ding et al. [66] synthetized tunable photoluminescent CDs by one pot hydrothermally synthesis (Fig.5a). Noteworthy, these CDs had comparable particle size and carbon core, but variable degree of oxidation of the surface state. Therefore, a gradual reduction in their band gaps and a red shift in their emission peaks from 440 to

Preprints (www.preprints.org) | NOT PEER-REVIEWED | Posted: 20 November 2020 doi:10.20944/preprints202011.0547.v1

625 nm (Fig.5b,c) was observed by increasing incorporation of oxygen species into their surface structures (fig.5d) [66].

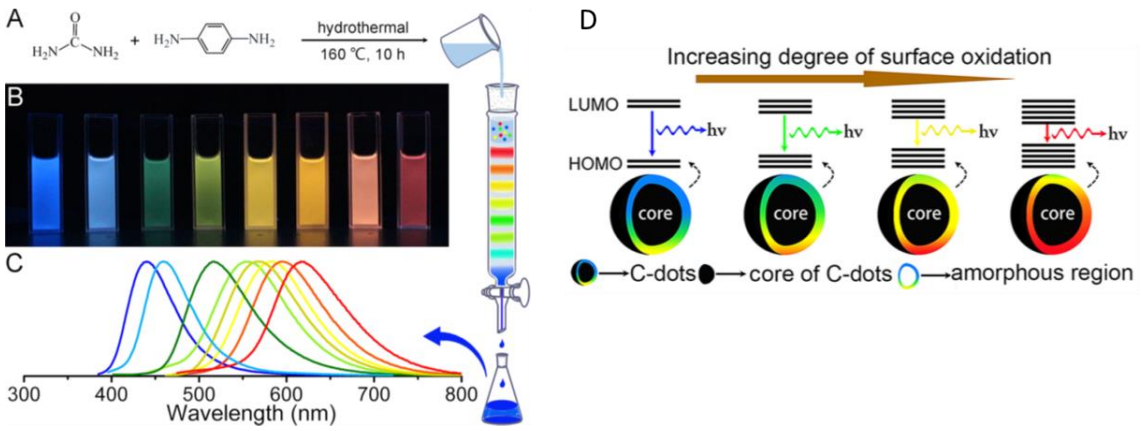

Figure 5. (a) One-pot synthesis and purification route for CDs with distinct PL characteristics. (b) Eight CD samples under 365 nm UV light. (c) Corresponding PL emission spectra. (d) Model for the tunable PL of CDs with different degrees of oxidation. Reprinted with permission from [66] Copyright 2015 American chemical society.

Also Miao et al. [67] hypothesized a similar mechanism. They modulate the CDs emission from 430 to 630 nm by controlling the degree of graphitization and the number of surface -COOH groups by changing the molar ratios of CA to urea at different temperatures (Fig.6). The increasing number of -COOH groups on the surface, increase the electronic delocalization and the emission wavelength is consequently red-shifted [64].

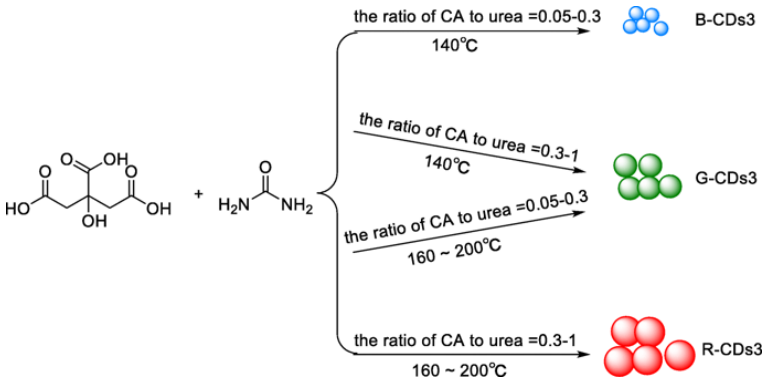

Figure 6. Multicolor-emitting CDs3 by using different molar ratios of CA to urea at different temperatures. The emission of CDs3 can be adjusted from 430 to 630 nm. The QYs of the three CDs3 of blue, green and red were 52.6%, 35.1% and 12.9%, respectively. Reprinted with permission from [64] Copyright (2019) Springer-Verlag.

Another relevant hypothesis for CDs emission is molecular luminophore-derived emission or molecular state emission. Small molecules or oligomeric luminophores could be produced during CD synthesis and these luminophores could be attached to the surface of CD backbones allowing CDs bright emission properties [68]. Song. et al.[69] studied the chemical structure and PL mechanism of CDs form CA and ethylenediamine (EDA). They proved the presence of a type of bright blue fluorophore and that the CDs emission was a result of small molecules, polymer clusters, and carbon cores. Indeed, the fluorophore may be attached to the carbon core, that may strongly affect the PL properties of the CDs

Preprints (www.preprints.org) | NOT PEER-REVIEWED | Posted: 20 November 2020 doi:10.20944/preprints202011.0547.v1

3 OLED-based Carbon dots

CDs with amazing properties such as optical characteristics and carbon's intrinsic merits of high stability, low-cost, and environment-friendliness, find a natural and practical application as components in OLED technology.

In the last decade the interest in OLED based on CDs (hereafter CD-OLEDs) has been growth and increasing number of research groups have started to investigate in this field.

We provide a recent advisor about CD-OLEDs, illustrating the dual employment of CDs as direct emitter, both as neat layer or as guest in host:guest systems, and as a charge regulating interlayer (Tab.1 and Fig.7). Particular attention will be devoted to the strategies used to prevent aggregation-induced quenching in the solid-state and to tune the emission colour. Notably, but out from the purpose of the present review, many groups used CDs also as a remote emitter, endowing blue commercial LEDs with a colour converting filter based on CDs embedded in poly(methyl-methacrylate) (PMMA) or other matrices. The blue LEDs emission was tuned from blue to red by altering the film thickness of the filter or the doping concentration of CDs [68, 69, 70].

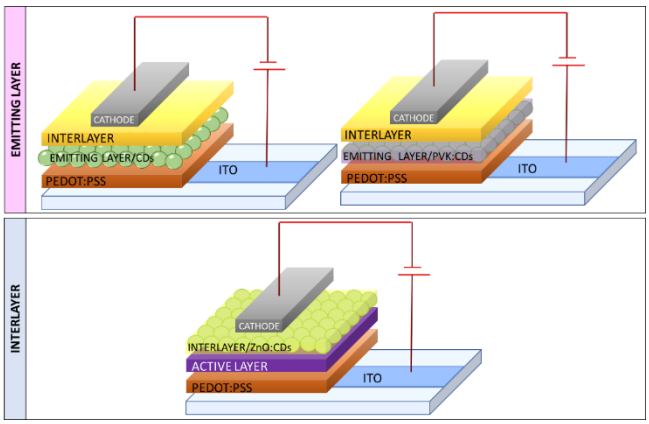

Figure 7 Scheme of the possible device architectures that incorporate CD as emitter or as interlayer.

Table 1. Summary of OLEDs incorporating a CDs layer.

starting materials	dimension (nm)/shape	ELMAX (nm)	LMAX (cd/m²)	ηc (Cd/A)	REF
CDs as emitter					
Phloroglucinol	triangular 1,9nm	476	1882	1,22	77
	2,4nm	510	4762	5,11	
	3nm	540	2784	2,31	
	3,9nm	602	2344	1,73	
citric acid and diaminonaphthalene.	quasi-spherical_2.4_lattice spacing 0.21nm	450	5240	2.6	63
Citric acid with 2,3-diaminonaphthalene	2,41nm(G)	536	2050	1.1	75

Preprints (www.preprints.org) | NOT PEER-REVIEWED | Posted: 20 November 2020 doi:10.20944/preprints202011.0547.v1

N,N-dimethyl-, N,N-diethyl-, and N,N-dipropyl-p-phenylenediamine	quasi-spherical_2.2 ± 0.31, 2.3 ± 0.28, 2.3 ± 0.26 nm_lattice spacing 0.21nm	605/434 612/435 616/435	5248–5909	3.65 3.85	76
human hair	2D array of CDs_2-6nm	498	350 700	0.22 0.2	78
anhydrous citric acid and hexadecylamine	spherical_2.0–2.5 nm_lattice spacing 0.22	558-550	339.5-455.2		74
anhydrous citric acid and hexadecylamine		474	569.8		75
CDs as interlayer					
ethylenediamine and citric acid		532	30 730	93.8	84
Ethanolamine		622	3500	0.63	80
banana leaves	4-6nm (quasi-spherical)	486			83

CDs as emitter

In 2011 Wang et al. [73] demonstrated the first white OLED (WOLED) originating from a single CDs component film. CDs, obtained by thermal carbonization of CA in hot octadecene with 1-hexadecylamine (HDA) as the passivation agent (Fig.8a), with a PLQY as high as 60 %, were incorporated as emitting layer in WOLEDs with a direct architecture (Fig.8b).

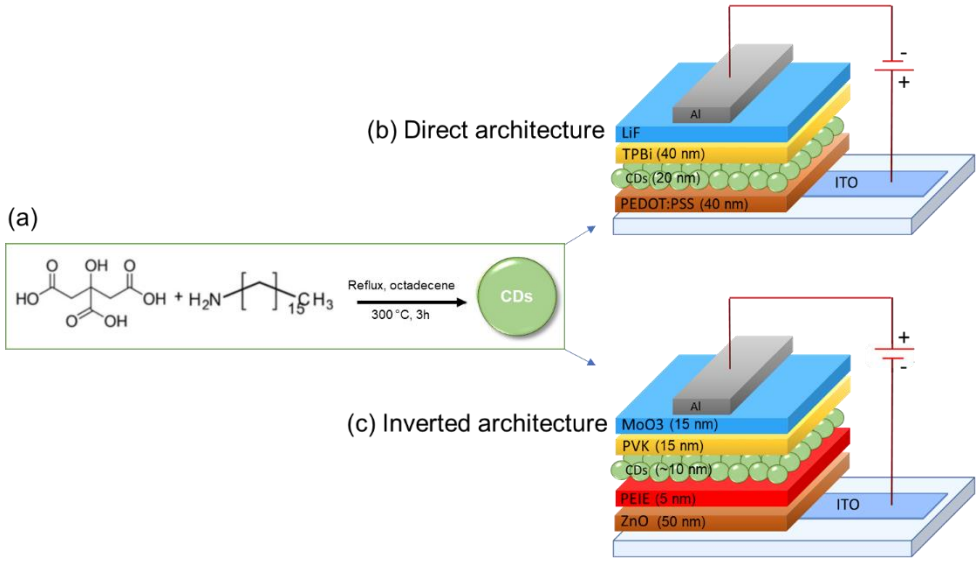

Figure 8: (a) Schematic representation of the CDs synthesis and typical devices architectures (b) direct [74] and (c) inverted [73] in which CDs are incorporated as emitters. Reprinted with permission from [67] Copyright (2019) The Royal Society of Chemistry.

Preprints (www.preprints.org) | NOT PEER-REVIEWED | Posted: 20 November 2020 doi:10.20944/preprints202011.0547.v1

Electrically driven WOLED featured electroluminescence (EL) peaked at 550 nm, with current density (J) of 160 mA/cm², a maximum luminance (L_{MAX}) output of 35 cd/m² and a current efficiency (η_c) of 0.022 cd/A. As shown in Fig.9c), the maximum external quantum efficiency (EQE), defined as the ratio between the number of emitted photons and the number of electrons injected into the device, was 0.083% at a J of 5 mA/cm².

Wang et al. reported that white light emission was associated with energy transfer among various emitting centre in the CDs, corresponding to different energy transitions.

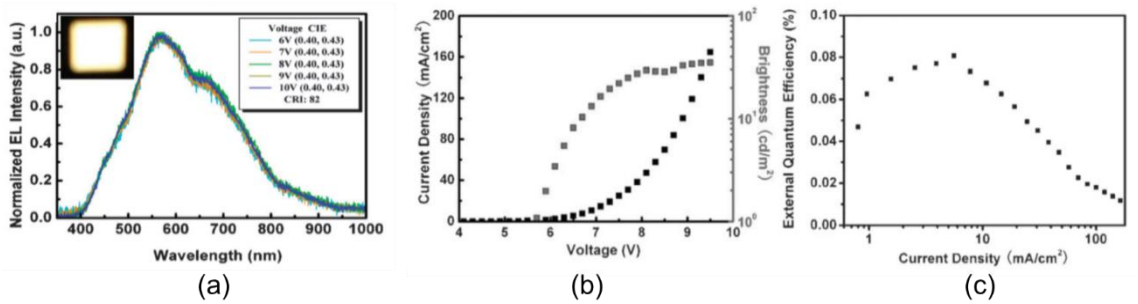

FIGURE 9. (a) Normalized electroluminescence spectra of direct architecture LEDs at applied bias voltages. Inset is the photograph of a white emission of our device (16 mm²) operating at 9 V. (b) Current density (J)–luminance (L)–voltage (V) characteristics of WOLEDs. (c) The dependence of external quantum efficiency (EQE) on J. Reproduced with permission from ref. [73] Copyright 2011 The Royal Society of Chemistry.

Paulo-Mirasol et al. [74] in 2019, by using CDs synthesized according to Wang conditions [73], demonstrated that the white light was not due to the charge transfer between the CDs, but it was the result of different recombination processes within the CDs . Indeed, they proposed two radiative photoluminescence mechanisms in the CDs involving different energies: one originating from the core and a second process that is faster and originates from the surface of CDs and the variation of the current injection controls the activation of the two radiative processes that happen inside the CDs. The combined emission from different energy states results in white light emission at an adequate current injection rate. Differently from Wang and colleagues, Paulo-Mirasol et al. manufactured OLEDs with an inverted architecture ITO/ZnO/PEIE/CDs/PVK/MoO_3/Au. and they modulated the thickness of CDs and polyvinylcarbazole (PVK, used as hole transporting layer or HTL) to optimize the performance of device obtaining a WOLEDs with L_{MAX} of 24 cd/m² and η_c 0.06 cd/A (Fig.10) compared with Wang (L_{MAX} 35 cd/m² and η_c of 0.022 cd/A).

Preprints (www.preprints.org) | NOT PEER-REVIEWED | Posted: 20 November 2020 doi:10.20944/preprints202011.0547.v1

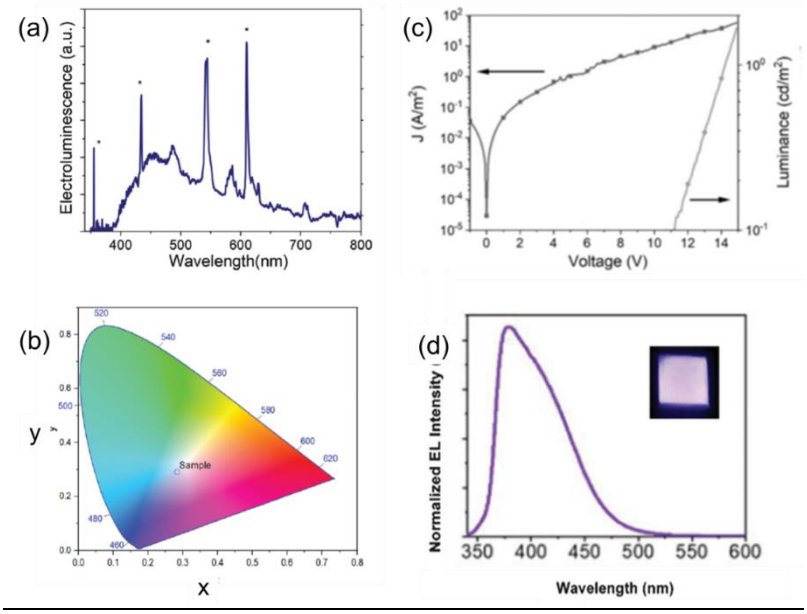

Figure 10. (a) The electroluminescence of the CD- LEDs at 8 V measured at room temperature (top). (b) CIE colour coordinates of LEDs with CDs as the single emitter. Current density and luminance versus applied voltage of the LED made without CDs. (d) digital picture of the device using PVK as the emissive layer at 12 V and the photoluminescent emission spectra of the device after excitation at 340 nm. Reproduced with permission from ref. [74] Copyright 2019 The Royal Society of Chemistry.

Ding and colleagues [66] proposed short-chain passivated CDs in fact short-chain cap shortens the distances of carriers from CDs, which probably facilitates the injection of carriers into CDs . Their CDs were synthesized via a one-step hydrothermal approach using phthalic acid and ethylenediamine, the resulting CDs aqueous solution featured a PLQY of 29.3% and good film-forming ability. CD-OLEDs were fabricated by a solution processing method and the devices exhibited a stable blue EL peak at 410 nm at 6-9 V. Despite the improvement of the carrier transfer ability of CDs achieved by the short-chain modification, the lower PLQY compared with that of long-chain passivated CDs and the not optimal device architecture (see energy barrier at the anode interface in Figure 11a), were the most probable explanation for the observed lower performance of devices (Fig.11b-d).

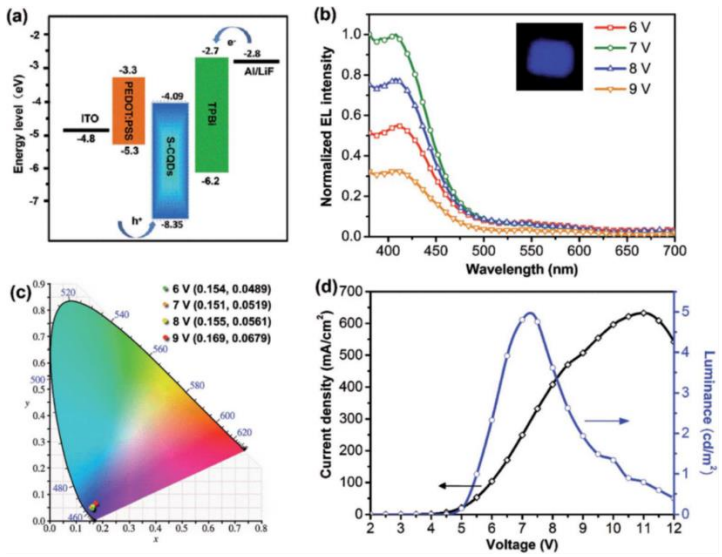

Preprints (www.preprints.org) | NOT PEER-REVIEWED | Posted: 20 November 2020 doi:10.20944/preprints202011.0547.v1

Figure 11. The schematic energy level diagram of the CD-LEDs. (b) Emission spectra under different working voltage (inset is the photograph of CD-LEDs under the working voltage of 7 V). (c) The CIE 1931 chromaticity coordinates of CD-LEDs under different working voltage. (d) The current density curve and brightness–voltage characteristics of CD-LEDs. Reproduced with permission from ref. 66 Copyright 2017 The Royal Society of Chemistry.

Zhang at al. in 2013 [75] observed for the first time, a multi-colored (bright blue, cyan, magenta and white) EL from CDs of the same size (3.3 nm). Such a switchable EL behavior has not previously observed in single nanomaterial emitting layer OLEDs. This all solution processed device consisted of a CDs emissive layer sandwiched between an organic HTL and an organic or inorganic ETL (electron transporting layer) with typical architecture ITO/PEDOT:PSS/PolyTPD/CDs/TPBI (were poly-TPD was poly- (N,N0-bis(4-butylphenyl)-N,N0-bis(phenyl) benzidine and TPBI 1,3,5-tris(N-phenylbenzimidazol-2-yl) benzene)) or ZnO/LiF/Al (Fig.12a). The devices structure was adjusted to control the J and therefore the EL spectra. By increasing LiF thickness from 1 at 5 nm, or replacing LiF and TPBi with ZnO, the emitted color changed, with the applied voltage, from blue, cyan, magenta, and white from the same carbon dots (Fig.12b,d).

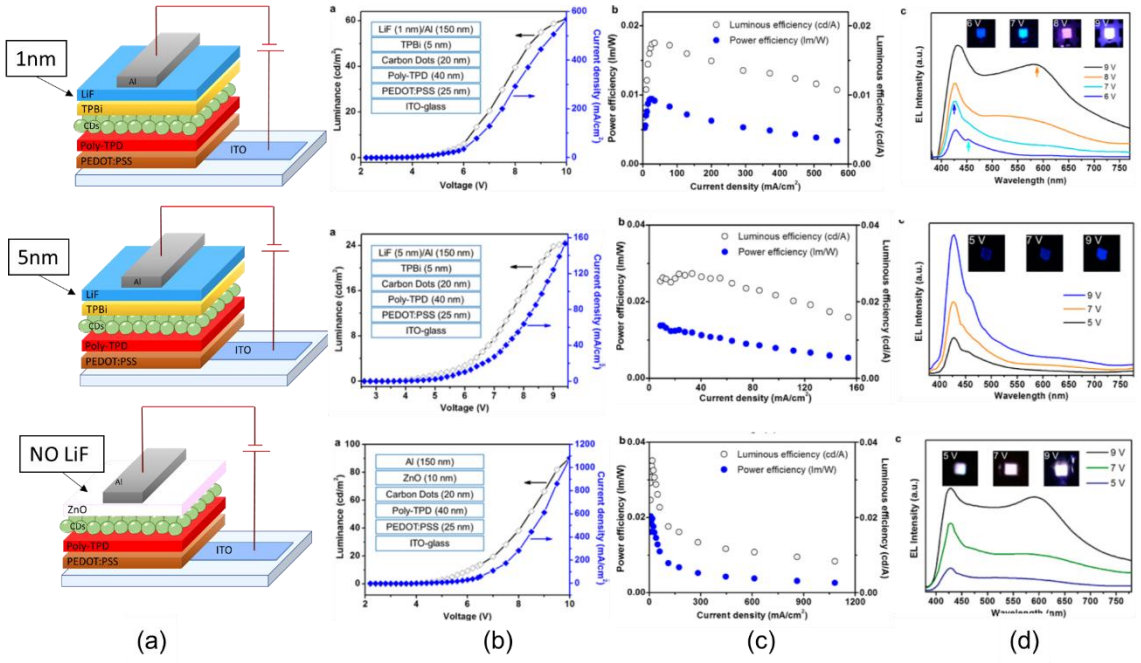

Figure 12. (a) Schematic representation of the CD-LED architectures together with (b) J and L versus V, (c) luminous and power efficiencies vs J, (d) EL spectra and images of the operating CD-LEDs at different applied voltage. Reproduced with permission from ref. [73] Copyright 2013 American Chemical Society.

The L_{MAX} obtained was 24 cd/m² for the blue-emitting OLED at low current injection. The L_{MAX} observed in devices incorporating ZnO nanoparticles was higher (90 cd/m²) thanks to the higher electron mobility of ZnO with respect to organic ETLs.

To solve the problem of quenching and aggregation of CDs since 2017 a host guest approach[76,77] was proposed with CDs as guest component and, usually, the PVK as a host matrix.

Yuan et al. [65] compared the performance of a neat CDs film and CDs dispersed in PVK. They reported the synthesis of bright multicolor fluorescent CDs (called MCBF-CDs) from blue to red with PLQY up to 75% for blue fluorescence through a facile solvothermal method. Their CDs were N-doped, highly surface passivated with a high degree of crystallinity. CDs were firstly employed directly as an active layer for monochromatic OLEDs with conventional simple architecture ITO/PEDOT:PSS/CDs/TPBI/Ca/Al (Fig.13a). Monochrome OLEDs featured blue (B), green (G),

Preprints (www.preprints.org) | NOT PEER-REVIEWED | Posted: 20 November 2020 doi:10.20944/preprints202011.0547.v1

yellow (Y), orange (O) and red (R) EL with peaks at 455, 536, 555, 585, 628 nm and CIE coordinates (0.19, 0.20), (0.31, 0.47), (0.37, 0.52), (0.46, 0.48) and (0.55, 0.41), respectively (Fig.13c,d). The EL spectra showed voltage-independent behavior as well as no temporal degradation, that are of great significance for display technology. In the B-OLEDs, L_{MAX} reached136 cd/m² with η_c of 0.084 cd/A (Fig.13b).

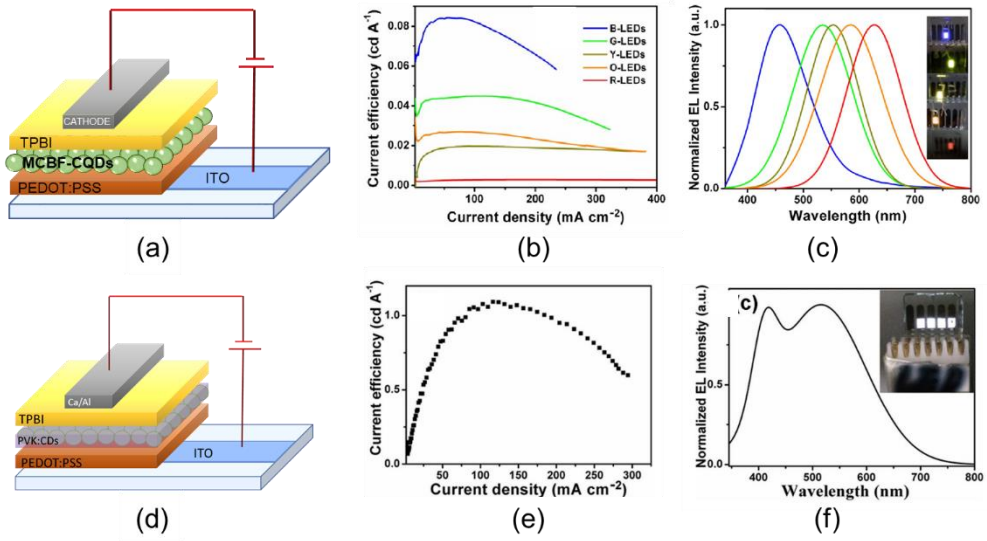

Figure 13. (a) Schematic representation of the MCBF-CDs –based devices architecture. (b) The current efficiency vs current density of MCBF-CDs-based monochrome electroluminescent OLEDs from blue to red. (c) The normalized EL spectra (in the inset, picture of the working devices) and (d) Schematic representation of the PVK:MCBF-CDs -based devices architecture. (e) The current efficiency vs current density of PVK:MCBF-CDs-based monochrome electroluminescent OLEDs from blue to red. (f) The normalized white EL spectra (in the inset, picture of the working devices) and (h) EL emission colour coordinates in the CIE 1931 chromaticity diagram. Reproduced with permission from ref. [63] Copyright 2016 Wiley-VCH.

In the devices incorporating a blend of green CD into a PVK polymer matrix (5wt.% ratio) with ITO/PEDOT:PSS/PVK:MCBF-CDs/TPBI/Ca/Al architecture (Fig.13d) Yuan et al. [65].reached a L_{MAX} and η_c as high as 2050 cd/m² and 1.1 cd/A with a low turn on voltage (V_{ON} = 3.9 V) (Fig.13e). In the broad EL spectrum two peaks were identified, centered at 410 and 517 nm and assigned to PVK and green MCBF-CD emission, (Fig.13f). The CIE coordinate of (0.30, 0.33), very close to ideal white, resulted from the energy transfer from PVK to CD and form the direct charge injection to CD.

In 2018 Xu et al. [78] synthesized oleophilic CDs, with a PLQY of 41%, by a one-pot microwave carbonization method (Fig.14a) to study the impact of CD aggregation as a limiting factor for the brightness of the CD-LEDs.

They fabricated CD-OLEDs, incorporating a neat CD active layer, with the simple architecture ITO/PEDOT:PSS/CD/TPBI/LiF/Al. The devices featured modest performance (Fig.14), with yellow emission peaked at 554 nm, L_{MAX} of 5.7 cd/m² at 10 V and CIE coordinates od (0.36, 0.42), most probably because of aggregation of the CDs.

Preprints (www.preprints.org) | NOT PEER-REVIEWED | Posted: 20 November 2020 doi:10.20944/preprints202011.0547.v1

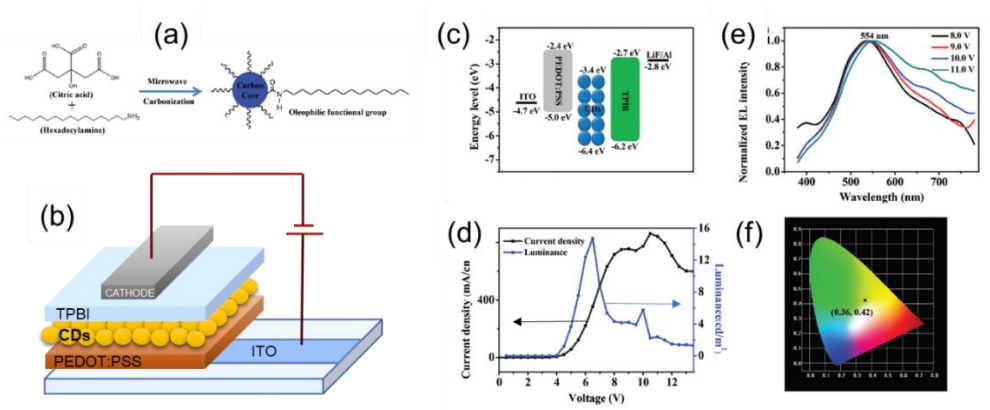

Figure 14. (a) Illustration of the route for the synthesis of CDs. Schematic representation of the devices architecture. The energy level diagram of the CD-LED. (b) The normalized EL spectra of the CD-LED at different driving voltages. (c) The current density–voltage–luminance (J–V–L) characteristics curve of the CD-LED. (d) The CIE coordinates of the CD-LED at the working voltage of 10.0 V. Reproduced with permission from ref. [78] Copyright 2018 The Royal Society of Chemistry.

The impact of CDs aggregation on the brightness of CD-OLEDs was studied also by blending the CDs in PVK. Yellow and white EL were observed by tuning the doping concentration of the active layer. The yellow EL, mainly derived from direct carrier trapping, reached L_{MAX} of 339.5 cd/m^2 with excellent color stability. The white CD-OLEDs exhibited a CRI value of 83 with CIE coordinates of (0.29, 0.33) and high L_{MAX} of 544.2 cd/m^2. The white EL resulted from the contemporary emission from PVK and CDs, and the good brightness was attributed to a suitable balance between holes and electrons in the emitting layer. (Fig.15) [78].

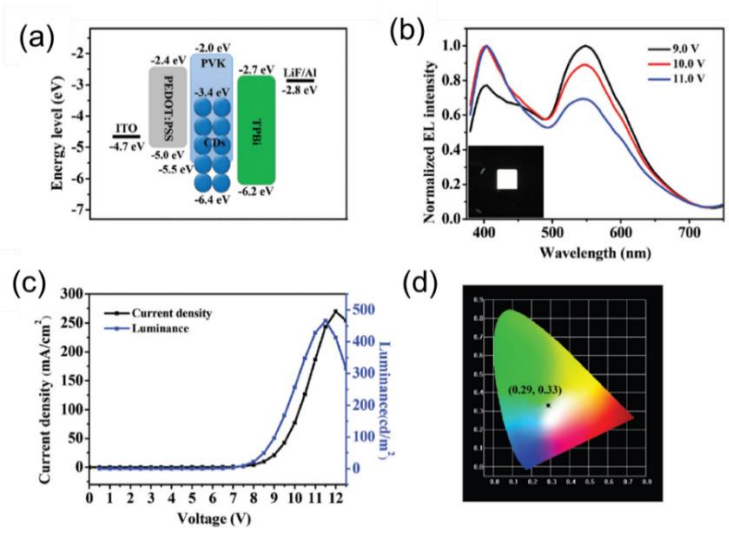

Figure 15. (a) The energy level diagram of the white CD-LED. (b) The normalized EL spectra of the white CD-LED at different voltages (in the inset, a photograph of the working device). (c) The J–V–L characteristics curve of the white CD-LED. (d) The CIE coordinates at a driving voltage of 11 V. Reproduced with permission from ref. [78] Copyright 2018 The Royal Society of Chemistry.

In the last 3 years the research on LEDs based on CDs increase and focalized, almost exclusively, on CDs dispersed in PVK as emitting layer. The next two articles showed that amination could be exploited to improve the performance of devices.

Yuan et al. [79] presented deep-blue light-emitting materials and devices based on CDs that outperform deep-blue emitting LEDs based on Cd^{2+}/Pb^{2+} materials. CDs were synthesized by solvothermal treatment using CA and DAN as precursors. To enables efficient high-color purity, an

Preprints (www.preprints.org) | NOT PEER-REVIEWED | Posted: 20 November 2020 doi:10.20944/preprints202011.0547.v1

additional surface amination step using ammonia liquor and hydrazine hydrate under high temperature was performed. This second step, decreasing the number of defects of CDs and thus suppresses non-radiative pathways, increases the quantum yield up to 70%.

CD-OLEDs were manufactured with the architecture ITO/PEDOT:PSS/TFB/PVK:CDs/TPBI/LiF/Al (Fig.16a). The corresponding energy level diagram (Fig.16b) show a mitigation of energy barrier for both electrons and holes injections thanks to the suitable selection of the different layers. The EL spectra remained at 440 nm across the range of voltage explored, and are in good agreement with the corresponding PL emission peaks indicating that an efficient energy transfer from PVK to CDs takes place. L and EQE as a function of V and J, respectively, are shown in Fig.16d,e. L_{MAX}, η_c and EQE reached remarkable values of 5240 cd/m^2, 2.6 cd/A and 4% respectively.

After operating continuously for 3 hours at 1000 cd/m^2, the OLED retained 50% of initial luminance (Fig.16f) without evident changes in EL spectrum.

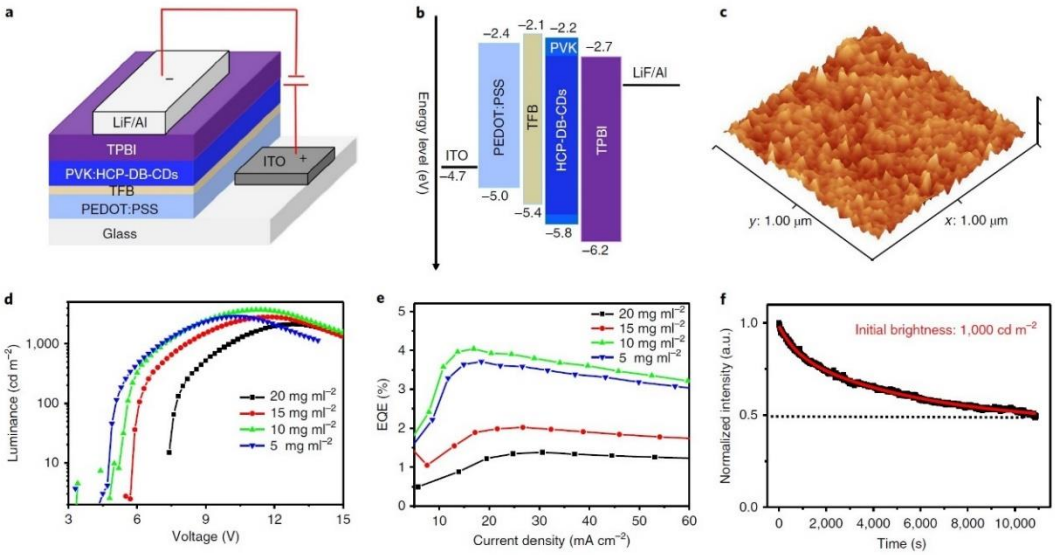

Figure 16. (a) PVK:CDs-based device structure, (b) energy level diagram, (c) AFM height image of PVK:CDs film, (d) Luminance–voltage (e) and EQE–current density characteristics, and (f) device stability. Reproduced with permission from ref. [79] Copyright 2020 Springer Nature group.

At the same time Jia and co-workers [80] demonstrated the effectiveness of the electron-donating group passivation strategy to impart in CD finely tuned properties for their application as emitters in CD-OLEDs. Specifically, they developed three efficient red-emissive CDs, by p-phenylenediamine and N,N-dimethyl-, N,N-diethyl-,and N,N-dipropyl obtaining CDs-NMe_2, -NEt_2, and -NPr_2, respectively (Fig.17a), with the aim to fabricate warm-light WOLEDs.

Thanks to theoretical investigations, they revealed that the CD emission originated from the rigid π-conjugated skeleton structure, while –NR_2 passivation played a key role in inducing charge transfer excited state in the π-conjugated structure to afford high PLQY (up to 86%).

Moreover, the polar –NR_2 groups are responsible for the good solubility of CDs in organic solvent and then processability by low-cost spin-coating technique. The CDs were dispersed in PVK.

Solution-processed OLEDs were fabricated with 9 wt.% CDs-NMe_2 (WOLEDs 1), -NEt_2 (WOLEDs 2), and -NPr_2 (WOLEDs 3) blended in PVK as emitting layer and the simple architecture ITO/PEDOT:PSS/PolyTPD/blend/TPBI/Ca/Al (Fig.17b). The WOLEDs generated warm-light with two main peaks (434/605, 435/612, and 453/616 nm for WLEDs-1,2,3 respectively, Fig.17d) attributed to emission from PVK and CDs. The corresponding CIE coordinates and correlate color temperatures were (0.379, 0.314)/3365 K, (0.383, 0.311)/3168 K, and (0.388, 0.309)/2987 K (Fig.17e).

Finally, WOLEDs-1,2,3 displayed voltages-stable EL spectra with a L_{MAX} in the range of 5248-5909 cd/m^2 (Fig.17f) and a η_c of 3.65-3.85 cd/A (Fig.17g).

Preprints (www.preprints.org) | NOT PEER-REVIEWED | Posted: 20 November 2020 doi:10.20944/preprints202011.0547.v1

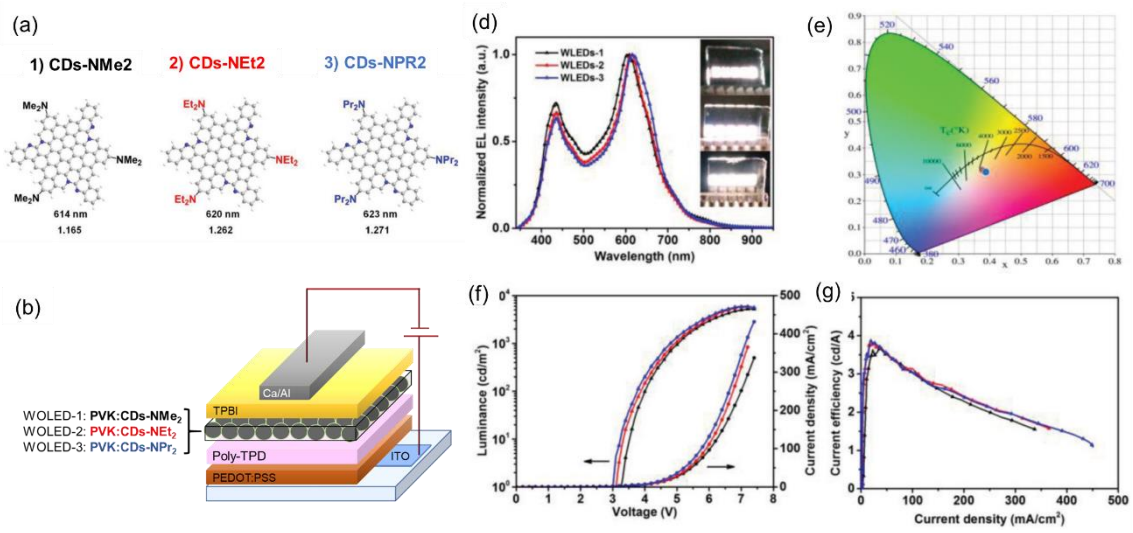

Figure 17. (a) CDs structures. (b) architecture of CD-WLEDs. (c) EL spectra, (c) operation photographs (insets in (a), from top to bottom), and corresponding CIE coordinates (d) of WLEDs-1, -2, and -3 under 7.0 V, respectively. (f) The J–V–L and (g) η_c of WLEDs-1 (black), -2 (red), and -3 (blue). Reproduced with permission from ref. [80] Copyright 2019 Wiley-VCH Verlag GmbH & Co.

Yuan et al. [81] recently addressed the issue of broad emission, usually observed in CD, which fundamentally limit their application in displays.

They synthetized multi-colored narrow bandwidth emission from triangular CDs (T-CDs). They demonstrated that the molecular purity and high crystallinity of the triangular CDs are indispensable to obtain the high color-purity. The triangular structure and the narrow bandwidth emission of triangular allowed to reduce dramatically electron-phonon coupling.

Conventional simple structure ITO/PEDOT:PSS/active layer/TPBI/Ca/Al (Fig.18b) was used for the fabrication of OLEDs from blue to red with the T-CDs blended in PVK as active emission layer. HOMO/LUMO energy levels of T-CDs were located within those of PVK then electrons and holes can be efficiently transferred from PVK to T-CDs emitter. The multi-colored OLEDs based on the T-CDs demonstrated high color-purity (FWHM of 30–39 nm) peaked at 476, 510, 540 and 602 nm for B-, G-, Y-, and R-LEDs respectively (Fig.16f-i), a η_c of 1.22–5.11 cd/A (Fig.18c) and L_{MAX} of 1882–4762 cd/m², rivalling the well-developed inorganic QDs-based LEDs. Finally, the LEDs exhibited outstanding stability (Fig.18e) which is of great significance foe display technology.

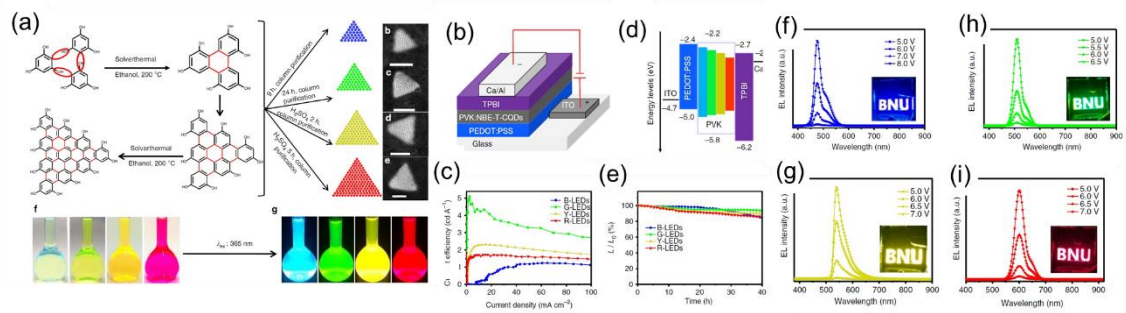

Figure 18. (a) Synthesis route of the NBE-T-CQDs by solvothermal treatment of PG triangulogen. Photographs of the T-CQDs ethanol solution under daylight (left) and fluorescence images under UV light (excited at 365 nm) (right) are included. (b) The device structure. (c) The current efficiency versus current density. (d) energy level diagram of the T-CQDs-based LEDs. (e) The stability plots of the B-, G-, Y-, and R-LED. EL spectra of the B- (f), G- (h), Y- (g), and R-LEDs (i) at different bias voltage, respectively (Insets are the operation photographs of the B-, G-, Y-, and R-LEDs with the logo of BNU). Reproduced with permission from ref. [81] Copyright 2019 Springer Nature group.

Preprints (www.preprints.org) | NOT PEER-REVIEWED | Posted: 20 November 2020 doi:10.20944/preprints202011.0547.v1

Singh and colleagues [82] fabricated the first flexible OLED (Fig.19a,b) based on CDs employing self-assembled 2D array of CDs embedded in PVK emission layer. The flexible device switched on at 4.3 V and exhibited a blue/cyan emission peaked at about 500 nm (comparable to PL emission, Fig.19c) with L_{MAX} of 350 cd/m² and η_c of 0.22 cd/A (Fig.19d,e), whereas the corresponding OLED device based on the rigid glass substrate featured a L_{MAX} of 700 cd/m² and η_c of 0.27 cd/A. Fig.19f shows the CD 2D island in the emitter layer.

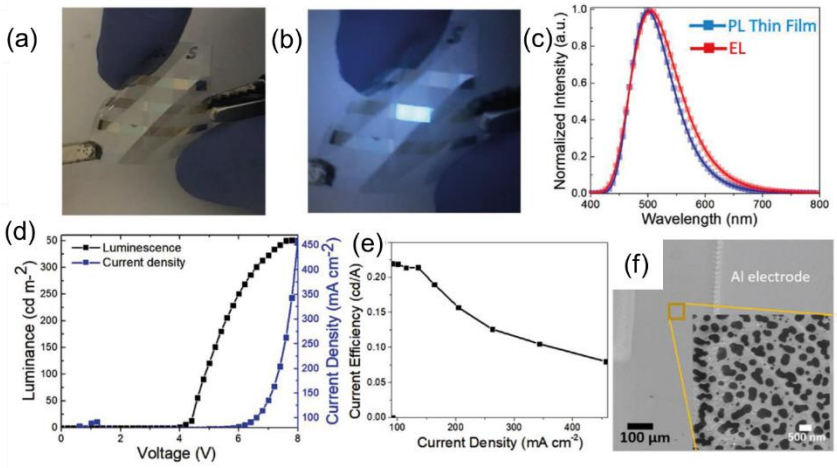

Figure 19. Picture of a flexible device: (a) off mode and (b) on mode. (c) The normalized EL spectra of the device and solid-state PL of a thin film. (d) L–I–V characteristic of the device. (e) Current efficiency versus current density. (f) CD 2D islands in the emitter layer. Reproduced with permission from ref. [82] Copyright 2020 Wiley-VCH Verlag GmbH & Co.

The host-guest energy transfer as main mechanism for CDs emission was exploited by Xu et al. [83] for the fabrication of solution processed blue CD-LEDs with ultrahigh brightness. Oleophylic CDs with PLQY of 41% were obtained using an anhydrous citric acid as carbon precursor and hexadecylamine as passivation agent by one-step microwave carbonization method. CDs with different doping concentrations were blended with PVK and incorporated into a simple and PEDOT-free device architecture ITO/PVK:CDs/TPBI/LiF/Al. The EL spectra of devices were dominated by the 474 nm CD emission peak with a contribution from PVK at around 410 nm. When the doping concentration was higher than 25 wt.%, a progressive weakening of PVK contribution in favour of an enhanced CD emission was observed. For 30 wt.% doping ratio, the L_{MAX} reached 569.8 cd/m² at a driving voltage of 12.5 V, and CIE coordinated of (0.22, 0.27) located in the blue light region. Also in this case, the long chain passivating ligands on the oleophylic CDs surface were responsible for the unideal transporting performance that limited the device efficiencies, but it should also be considered that the devices does not contain the commonly employed PEDOT:PSS layer.

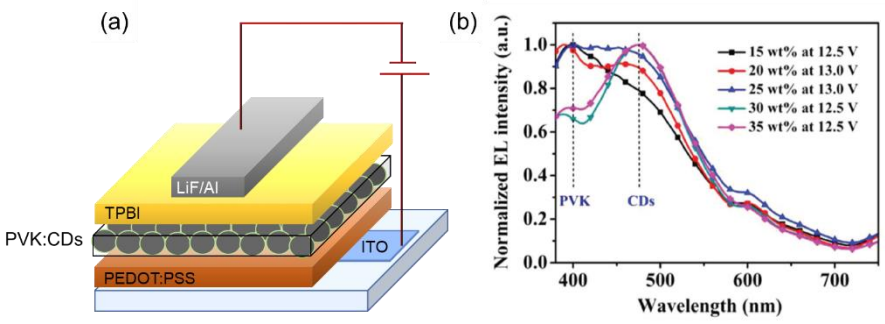

Figure 20. (a) Device architecture and normalized EL spectra for different CD doped devices. Reproduced with permission from ref. [83] Copyright 2020 Wiley-VCH Verlag GmbH & Co

Preprints (www.preprints.org) | NOT PEER-REVIEWED | Posted: 20 November 2020 doi:10.20944/preprints202011.0547.v1

CDs as charge regulating Interlayer

The possibility to tune CD's energy levels and intrinsic charge carrier transport, allows and alternative use of CD besides the incorporation as emitting layer. The following paragraph demonstrated that CDs, employed as interlayer (like interfacial layer also called charge regulating layer) in device's architectures based on different class of emitters, may improve the overall performance of the LEDs. The CD layer was incorporated both as ETL and HTL in either direct and inverted LEDs architecture (Fig.7b,c).

In 2017 Park et al. [84] explore the possibility to enhance performance of nanocrystal LEDs (NC-LEDS) based on quantum dots active layer. NC-LEDs typically take advantage of the incorporation of organic or inorganic interfacial layers as charge regulators to ensure charge balancing and high performance [85]. They investigated the roles played by CDs N-doped interlayer inserted by spin-coating between the PVK as HTL and the QD emitting layer (core/shell CdSe/CdS) [86,87]. In fact, QD-LEDs basically consisted of a multilayer architecture ITO/PEDOT:PSS/PVK/with or without N-CD/QD/ZnO/Al (Type A and B, Fig.21a). They showed that CDs HTL decrease the highest hole barrier height thus leading to a more balanced carrier injection and improved hole conduction capability. Moreover, they demonstrate that CDs interlayer acted as a resonant energy donor layer to the QD layer.

Both type A and B devices exhibited good electrical rectification, but the leakage current of type A QD-LEDs was significantly suppressed by inserting the N-CD layer (see lower J for type A device with respect to type B ones in the ohmic range below 0.5 V in Fig.21c). Noteworthy, the L_{MAX} observed in LED incorporating CDs outperformed type B LEDs, showing 3500 and 20 cd/m^2, and the η_c were 0.63 and 0.044 cd/A, respectively (Fig.21d,e). EL of both types of LEDs was dominated by the emission peak at 622 nm under applied voltage > 4 V (Fig.21f) with CIE coordinates of (0.66, 0.33) corresponding to the highly pure red emission (Fig.21g).

Preprints (www.preprints.org) | NOT PEER-REVIEWED | Posted: 20 November 2020 doi:10.20944/preprints202011.0547.v1

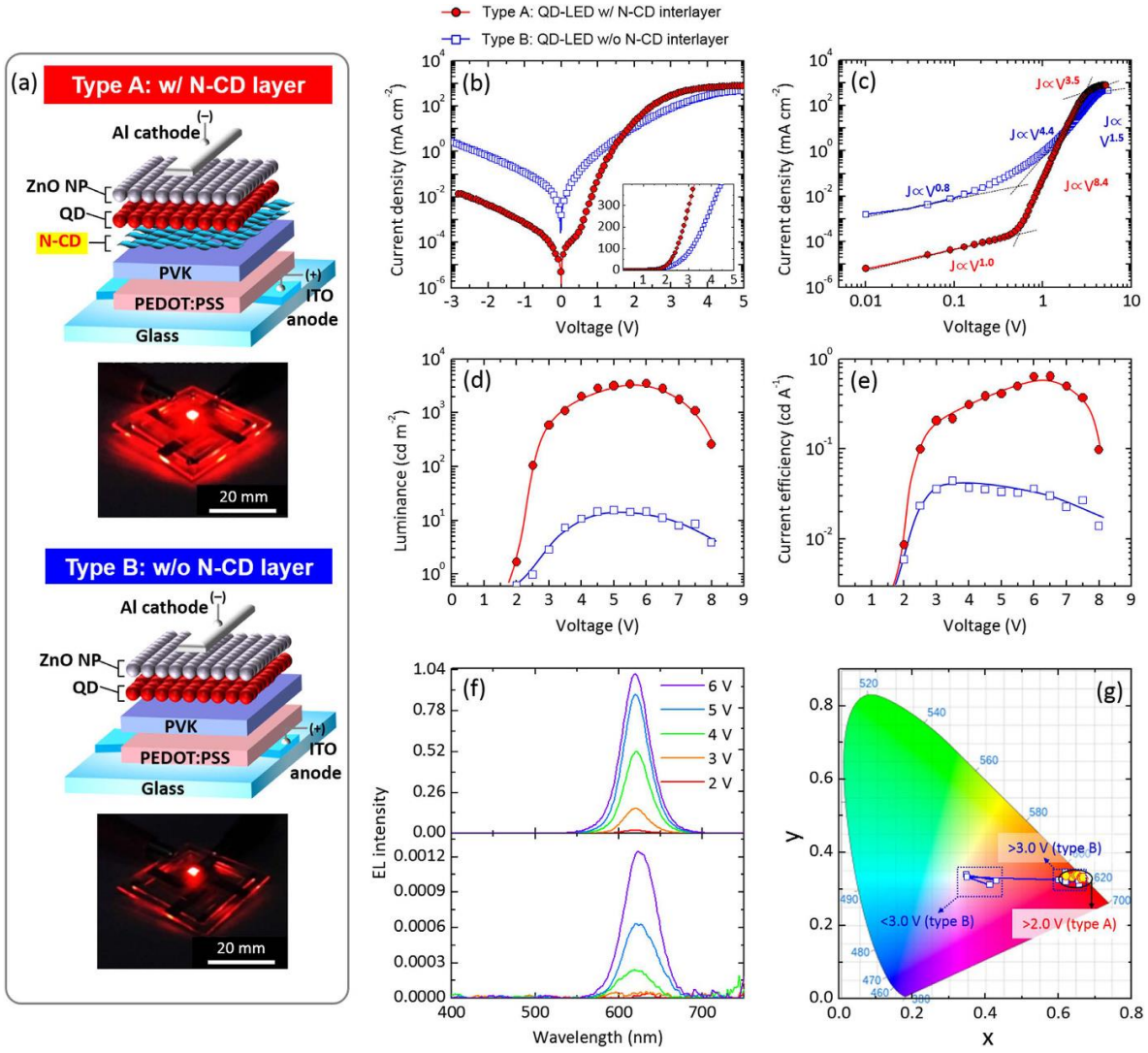

Figure. 21. (a) Schematic illustrations depicting the structures of solution-processed QD-LEDs. The photographs of red emission from both types of QD-LEDs is reported. (b) J–V characteristic curves. Inset is plotted in a linear scale at forward applied voltages. (c) J–V characteristic curves plotted on double-logarithmic axes. (d) Luminance and (e) Current efficiency plotted as a function of applied bias voltage. (f) EL spectra of the N-CD-inserted QD-LED (upper panel) and the control QD-LED (lower panel) at diverse applied voltages. (g) CIE coordinates of EL emission colours measured at various applied bias voltages of 2.0–8.0 V. Reproduced with permission from ref. [84] Copyright 2019 Springer Nature group.

In a very recently publication Paulo-Mirasol et al. [88] described the use CDs as HTL, but in an inverted LED architecture. They synthetized four N-doped CDs by citric acid as precursor of carbon skeleton and p-phenylenediamine, EDA, urea and HDA as precursor of capping ligand and show that the nature of the capping ligand influences directly the optoelectronic properties of CDs (Tab.2). The architecture of the device consisted of ZnO nanoparticles layer directly deposited on ITO, of an emissive conjugated polymer, the well-known and commercially available poly (9,9-dioctylfluorene-alt- benzothiazole or F8BT, and of the CDs (Fig.22a) as HTL. The devices were completed by Au anode.

The LEDs displayed moderate L values, but always clearly superior to the control CD-free device (Fig.22b). In the case of EDA capping, the V_{ON} was very low, which indicates the existence of an excellent charge injection capability. On the other hand, devices prepared with urea and HAD CDs showed the highest luminance.

Preprints (www.preprints.org) | NOT PEER-REVIEWED | Posted: 20 November 2020 doi:10.20944/preprints202011.0547.v1

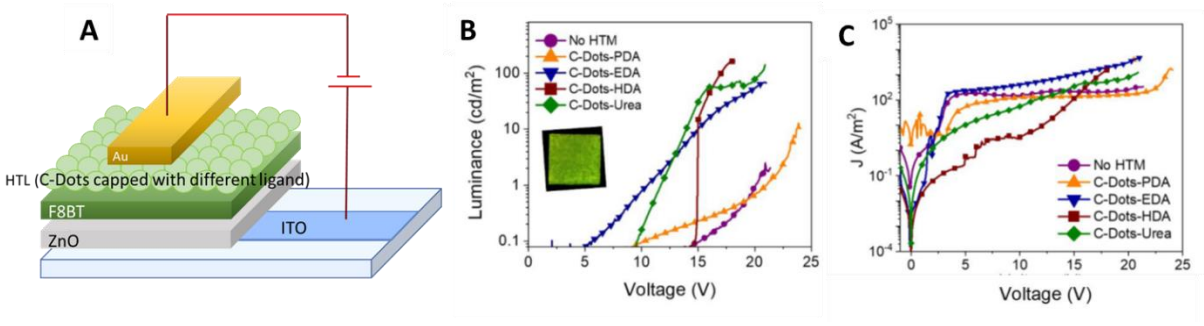

Figure 22. (a) device architecture, (b) luminance vs. applied bias (the inset shows a device working) and (c) current density vs applied bias for the inverted LEDs prepared using the CDs in the selective contact for holes. Reproduced with permission from ref. [88] Copyright 2019 American Chemical Society.

Table 2. Summarized most relevant parameters of devices from ref. 82, including values obtained for a control device without HTL.

Hole transport materials	Capping ligand hole mobility[a)]	L_{MAX} (cd/m²)	η_c (cd/A)
C-Dots-EDA	2.41±0.60	70	$2x10^{-3}$
C-Dots-PDA	1.5±0.47	13	$9x10^{-4}$
C-Dots-HDA	85.4±1.7	174	$8x10^{-4}$
C-Dots-Urea	2.92±0.32	146	$2x10^{-3}$
No HTM (control)	/	2	$5x10^{-4}$

a) space charge limited current hole mobility measured in hole-only devices.

Alam et al.[89] reported the use of CDs synthesized with one step hydrothermal process using banana leaf precursor, as ETL in direct architecture LEDs with polyfluorene derivative as emitting layer (Fig.23a). The introduction of CD as ETL reduces the barrier for electron injection which in turn lowered the V_{ON}. The EL spectra showed dominant peaks typical of PFO, but slightly red-shifted compared to literature.

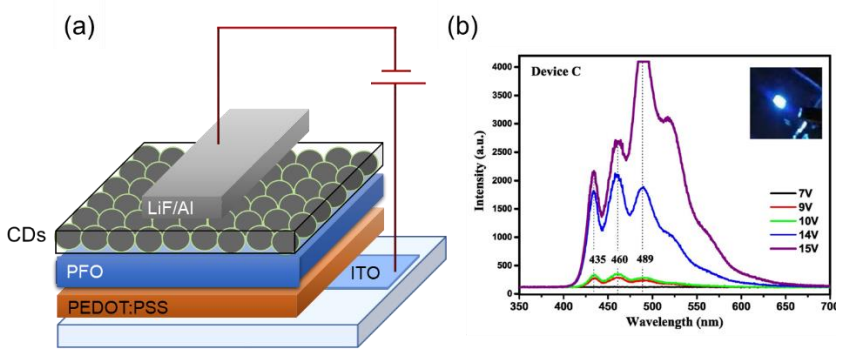

Figure 23. (a) device architecture, (b) EL spectra as a function of operating voltage. Reproduced with permission from ref. [89] Copyright 2019 Wiley-VCH Verlag GmbH & Co.

Zang et al. [90] demonstrated that stable, abundant, and easily-tosynthesize CDs are suitable as solution processable thin transparent films, serving as the cathode surface modifier in inverted LED architecture. This CD ETL can minimize the charge injection/extraction energy barrier, improve the interface contact property, and smooth the electron transport pathways in various optoelectronic devices such as perovskite solar cells and QD-LEDs. A series of CDs with varying content of either amine or carboxyl groups at their surface were synthesized using varying ratios of common precursors CA and EDA. Thanks to film consisting in a blend of CDs in ZnO, the WF of commonly used ITO substrates was modified over a broad range to become suitable as electron injection

Preprints (www.preprints.org) | NOT PEER-REVIEWED | Posted: 20 November 2020 doi:10.20944/preprints202011.0547.v1

electrode in inverted device architecture (Fig.24a,b). Specifically, CD modifiers with abundant amine groups reduced the ITO's WF from 4.64 to 3.42 eV, while those with abundant carboxyl groups increased it to 4.99 eV. Regarding the LED technology, they manufactured inverted architecture $CsPbI_3$ QD-LEDs with EQE increased, thanks to the incorporation of the CD layer, from 4.8% to 10.3% and the L_{MAX} increases from 951 to 1605 cd/m² (Fig.24c,e) and that of CdSe/ZnS QD- LEDs increases from 8.1% to 21.9% and η_c increases from 34.7 cd/A at 93.8 cd/A (Fig.24d,f) .

The proposed approach may hold true for CDs with other surface functional groups, which guides us toward more ideal interface materials, and offering chances to lower the production costs of various solution-processed optoelectronic devices with an improved performance.

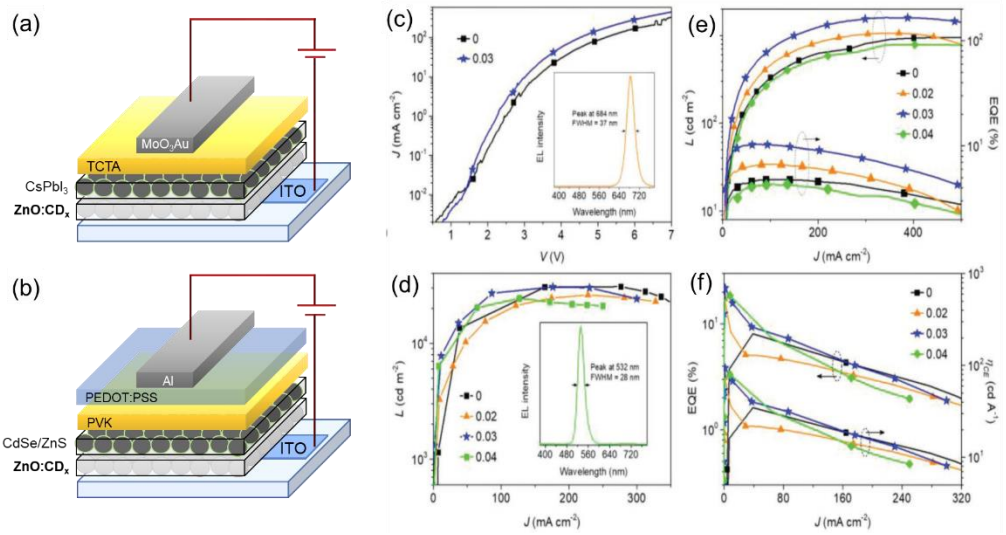

Figure 23. (a) $CsPbI_3$ and (b) CdSe/ZnS QD-LEDs devices architectures. (c) Current density versus voltage of $CsPbI_3$ QD LEDs with or without CDs (concentration 0.03 mg mL−1 in ZnO, CD_x x being molar ratio of CA and EDA precursors) interface modifier; the EL spectrum of the LED employing the CDs (0.03 mg mL−1) modifier is given as an inset. (e) Luminance and EQE versus current density of $CsPbI_3$ QD LEDs modified with different concentrations of $CD_{0.33}$ as given on the frame (in mg/mL). (d) Luminance versus current density of CdSe/ZnS QD LEDs modified with different concentrations of CDs as given on the frame (in mg/mL); the EL spectrum of the LED employing the CDs (concentration 0.03 mg/mL) modifier is given as an inset. (f) EQE and current efficiency versus current density of CdSe/ZnS QD LEDs with or without CDs modifier introduced at different concentrations (in mg/mL) provided on the frame. Reproduced with permission from ref. [90] Copyright 2019 WILEY-VCH Verlag GmbH & Co.

4 Summary and Outlook

CDs are materials with a great potential from multiple points of view. In fact, despite being relatively young materials, whose discovery is placed between 2004 and 2006, their development has already led to particularly encouraging results in many disciplines including biosensing, photonics and optoelectronics.

The interest in this class of materials is both academic and applicative. In fact, numerous efforts have been made to understand and modulate their chemical and physical properties and nevertheless, although different mechanisms have been highlighted, much remains to be done, especially in reproducibility and in the deep understanding of their size, shape, composition/doping properties dependence.

With regard to their application in OLEDs, as here reported, they have been used both as active layers and as charge regulation layers.

As active layers have been used dispersed in the matrix to avoid aggregation quenching, but also as neat film, leading to increasingly encouraging results mostly when their surface was passivated by hexadecylamine (HDA) agent [71, 82].

Recently, CDs have been tested as charge regulating layer (both for holes and for electrons), in either direct or inverted device's architectures, highlighting their great versatility linked to the huge number of possible modifications which, as we have pointed out, are related to composition, shape, size, and surface groups. Importantly, CDs used as ETL in OLED with direct architecture were synthetized with one step hydrothermal process using banana leaf as raw material.

In our opinion, the importance of these materials consists in the possibility of declining them to the concept of safe-by-design which is substantially at the basis of the circular economy (Fig. 1A).

To promote sustainability in the electronics industry, a paradigm shift needs to occur in economic practices from linear to circular. According to the Ellen McArthur Foundation, new electronics must be designed for sustainability from the get-go [91].

Technical performance is not the only driving force for the design but also the use of sustainable precursor (from waste or renewable materials), biodegradability, toxicity, synthetic methodology, production of toxic waste are only some of key parameters to be taken into consideration.

In this perspective, although CDs are currently still very far from the performance of other active materials commonly used in LED and OLED such as metallic quantum dots or organic semiconductors, in a circular perspective they are already able to meet some fundamental requirements.

For this reason, we hope that this review can offer a contribution and be a source of inspiration for the transition towards a "circular organic electronics".

Acknowledgements

This work was carried out with the financial support of Regione Lombardia Project "Piattaforma tecnologica per lo sviluppo di sonde innovative in ambito biomedicale" (ID 244356). U.G. thanks the MIUR-PRIN project Prot. 20172M3K5N.

Conflicts of Interest

The authors declare no conflict of interest.

References

1. Baldé, C.P.; Forti, V.; Gray, V.; Kuehr, R.; Stegmann, P.; International Telecommunication Union; United Nations University; International Solid Waste Association *The global e-waste monitor 2017 : quantities, flows, and resources*; ISBN 9789280890532.

2. Ostroverkhova, O. Organic Optoelectronic Materials: Mechanisms and Applications. *Chem. Rev.* 2016, *116*, 13279–13412.

3. Forrest, S.R.; Thompson, M.E. Introduction: Organic electronics and optoelectronics. *Chem. Rev.* 2007, *107*, 923–925.

4. Georges Hadziioannou (Editor), G.G.M. (Editor) *Semiconducting Polymers: Chemistry, Physics and Engineering, 2nd Edition, Two-Volume Set | Wiley*; Georges Hadziioannou (Editor), G.G.M. (Editor), Ed.; wiley, 2006; ISBN 978-3-527-31271-9.

5. Zvezdin, A.; Di Mauro, E.; Rho, D.; Santato, C.; Khalil, M. En route toward sustainable organic electronics. *MRS Energy Sustain.* **2020**, *7*, doi:10.1557/mre.2020.16.

6. Giovanella, U.; Betti, P.; Bolognesi, A.; Destri, S.; Melucci, M.; Pasini, M.; Porzio, W.; Botta, C. Core-type polyfluorene-based copolymers for low-cost light-emitting technologies. *Org. Electron.* **2010**, *11*, doi:10.1016/j.orgel.2010.09.009.

7. Irimia-Vladu, M. "Green" electronics: Biodegradable and biocompatible materials and devices for sustainable future. *Chem. Soc. Rev.* 2014, *43*, 588–610.

8. Yan, L.; Zhao, F.; Wang, J.; Zu, Y.; Gu, Z.; Zhao, Y. A Safe-by-Design Strategy towards Safer Nanomaterials in Nanomedicines. *Adv. Mater.* 2019, *31*.

9. Gomulya, W.; Derenskyi, V.; Kozma, E.; Pasini, M.; Loi, M.A. Polyazines and Polyazomethines with Didodecylthiophene Units for Selective Dispersion of Semiconducting Single-Walled Carbon Nanotubes. *Adv. Funct. Mater.* **2015**, *25*, 5858–5864, doi:10.1002/adfm.201502912.

10. Xu, X.; Ray, R.; Gu, Y.; Ploehn, H.J.; Gearheart, L.; Raker, K.; Scrivens, W.A. Electrophoretic analysis and purification of fluorescent single-walled carbon nanotube fragments. *J. Am. Chem. Soc.* **2004**, *126*, 12736–12737, doi:10.1021/ja040082h.

11. Sun, Y.P.; Zhou, B.; Lin, Y.; Wang, W.; Fernando, K.A.S.; Pathak, P.; Meziani, M.J.; Harruff, B.A.; Wang, X.; Wang, H.; et al. Quantum-sized carbon dots for bright and colorful photoluminescence. *J. Am. Chem. Soc.* **2006**, *128*, 7756–7757, doi:10.1021/ja062677d.

12. Xiao, L.; Sun, H. Novel properties and applications of carbon nanodots. *Nanoscale Horizons* 2018, *3*, 565–597.

13. Li, X.; Rui, M.; Song, J.; Shen, Z.; Zeng, H. Carbon and Graphene Quantum Dots for Optoelectronic and Energy Devices: A Review. *Adv. Funct. Mater.* **2015**, *25*, 4929–4947, doi:10.1002/adfm.201501250.

14. Semeniuk, M.; Yi, Z.; Poursorkhabi, V.; Tjong, J.; Jaffer, S.; Lu, Z.H.; Sain, M. Future Perspectives and Review on Organic Carbon Dots in Electronic Applications. *ACS Nano* **2019**, *13*, 6224–6255, doi:10.1021/acsnano.9b00688.

15. Campuzano, S.; Yáñez-Sedeño, P.; Pingarrón, J.M. Carbon dots and graphene quantum dots in electrochemical biosensing. *Nanomaterials* 2019, *9*.

16. Liu, M.L.; Chen, B. Bin; Li, C.M.; Huang, C.Z. Carbon dots: Synthesis, formation mechanism, fluorescence origin and sensing applications. *Green Chem.* 2019, *21*, 449–471.

17. Wang, Y.; Hu, A. Carbon quantum dots: Synthesis, properties and applications. *J. Mater. Chem. C* **2014**, *2*, 6921–6939, doi:10.1039/c4tc00988f.

18. Gayen, B.; Palchoudhury, S.; Chowdhury, J. Carbon dots: A mystic star in the world of nanoscience. *J. Nanomater.* 2019, *2019*.

19. Chan, K.K.; Yap, S.H.K.; Yong, K.T. Biogreen Synthesis of Carbon Dots for Biotechnology and Nanomedicine Applications. *Nano-Micro Lett.* 2018, *10*, 72–72.

20. Zuo, J.; Jiang, T.; Zhao, X.; Xiong, X.; Xiao, S.; Zhu, Z. Preparation and Application of Fluorescent Carbon Dots. *J. Nanomater.* **2015**, *2015*, doi:10.1155/2015/787862.

21. Pal, A.; Sk, M.P.; Chattopadhyay, A. Recent advances in crystalline carbon dots for superior application potential. *Mater. Adv.* **2020**, *1*, 525–553, doi:10.1039/d0ma00108b.

22. Sun, Y.P.; Zhou, B.; Lin, Y.; Wang, W.; Fernando, K.A.S.; Pathak, P.; Meziani, M.J.; Harruff, B.A.; Wang, X.; Wang, H.; et al. Quantum-sized carbon dots for bright and colorful photoluminescence. *J. Am. Chem. Soc.* **2006**, *128*, 7756–7757, doi:10.1021/ja062677d.

23. Li, X.; Wang, H.; Shimizu, Y.; Pyatenko, A.; Kawaguchi, K.; Koshizaki, N. Preparation of carbon quantum dots with tunable photoluminescence by rapid laser passivation in ordinary organic solvents. *Chem. Commun.* **2011**, *47*, 932–934, doi:10.1039/c0cc03552a.

24. Yang, Z.C.; Wang, M.; Yong, A.M.; Wong, S.Y.; Zhang, X.H.; Tan, H.; Chang, A.Y.; Li, X.; Wang, J. Intrinsically fluorescent carbon dots with tunable emission derived from hydrothermal treatment of glucose in the presence of monopotassium phosphate. *Chem. Commun.* **2011**, *47*, 11615–11617, doi:10.1039/c1cc14860e.

25. Hu, S.; Liu, J.; Yang, J.; Wang, Y.; Cao, S. Laser synthesis and size tailor of carbon quantum dots. *J. Nanoparticle Res.* **2011**, *13*, 7247–7252, doi:10.1007/s11051-011-0638-y.

26. Tarasenka, N.; Stupak, A.; Tarasenko, N.; Chakrabarti, S.; Mariotti, D. Structure and Optical Properties of Carbon Nanoparticles Generated by Laser Treatment of Graphite in Liquids. *ChemPhysChem* **2017**, *18*, 1074–1083, doi:10.1002/cphc.201601182.

27. De, B.; Karak, N. A green and facile approach for the synthesis of water soluble fluorescent carbon dots from banana juice. *RSC Adv.* **2013**, *3*, 8286–8290, doi:10.1039/c3ra00088e.

28. Zhu, S.; Meng, Q.; Wang, L.; Zhang, J.; Song, Y.; Jin, H.; Zhang, K.; Sun, H.; Wang, H.; Yang, B. Highly photoluminescent carbon dots for multicolor patterning, sensors, and bioimaging. *Angew. Chemie - Int. Ed.* **2013**, *52*, 3953–3957, doi:10.1002/anie.201300519.

29. Dong, Y.; Pang, H.; Yang, H. Bin; Guo, C.; Shao, J.; Chi, Y.; Li, C.M.; Yu, T. Carbon-based dots co-doped with nitrogen and sulfur for high quantum yield and excitation-independent emission. *Angew. Chemie - Int. Ed.* **2013**, *52*, 7800–7804, doi:10.1002/anie.201301114.

30. Chen, Y.; Lian, H.; Wei, Y.; He, X.; Chen, Y.; Wang, B.; Zeng, Q.; Lin, J. Concentration-induced multi-colored emissions in carbon dots: Origination from triple fluorescent centers. *Nanoscale* **2018**, *10*, 6734–6743, doi:10.1039/c8nr00204e.

31. Ehrat, F.; Bhattacharyya, S.; Schneider, J.; Löf, A.; Wyrwich, R.; Rogach, A.L.; Stolarczyk, J.K.; Urban, A.S.; Feldmann, J. Tracking the Source of Carbon Dot Photoluminescence: Aromatic Domains versus Molecular Fluorophores. *Nano Lett.* **2017**, *17*, 7710–7716, doi:10.1021/acs.nanolett.7b03863.

32. Bao, L.; Liu, C.; Zhang, Z.L.; Pang, D.W. Photoluminescence-tunable carbon nanodots: Surface-state energy-gap tuning. *Adv. Mater.* **2015**, *27*, 1663–1667, doi:10.1002/adma.201405070.

33. Zhang, J.; Su, Z.C.; Cui, Y.; Hu, G.; Tang, Y.L.; Gan, Z.X.; Yang, L.; Lao, X.Z.; Bao, Y.T.; Xu, S.J. The roles of self-absorption and radiative energy transfer in photoluminescence of N-doped carbon nanodots in solution. *AIP Adv.* **2019**, *9*, 035135, doi:10.1063/1.5078443.

34. Khan, S.; Gupta, A.; Verma, N.C.; Nandi, C.K. Time-Resolved Emission Reveals Ensemble of Emissive States as the Origin of Multicolor Fluorescence in Carbon Dots. *Nano Lett.* **2015**, *15*, 8300–8305, doi:10.1021/acs.nanolett.5b03915.

35. Zhu, S.; Zhang, J.; Liu, X.; Li, B.; Wang, X.; Tang, S.; Meng, Q.; Li, Y.; Shi, C.; Hu, R.; et al. Graphene quantum dots with controllable surface oxidation, tunable fluorescence and up-conversion emission. *RSC Adv.* **2012**, *2*, 2717, doi:10.1039/c2ra20182h.

36. Wang, X.; Qu, K.; Xu, B.; Ren, J.; Qu, X. Microwave assisted one-step green synthesis of cell-permeable multicolor photoluminescent carbon dots without surface passivation reagents. *J. Mater. Chem.* **2011**, *21*, 2445, doi:10.1039/c0jm02963g.

37. Yang, S.T.; Wang, X.; Wang, H.; Lu, F.; Luo, P.G.; Cao, L.; Meziani, M.J.; Liu, J.H.; Liu, Y.; Chen, M.; et al. Carbon dots as nontoxic and high-performance fluorescence imaging agents. *J. Phys. Chem. C* **2009**, *113*, 18110–18114, doi:10.1021/jp9085969.

38. Wang, K.; Gao, Z.; Gao, G.; Wo, Y.; Wang, Y.; Shen, G.; Cui, D. Systematic safety evaluation on photoluminescent carbon dots. *Nanoscale Res. Lett.* 2013, *8*, 1–9.

39. Dias, C.; Vasimalai, N.; P. Sárria, M.; Pinheiro, I.; Vilas-Boas, V.; Peixoto, J.; Espiña, B. Biocompatibility and Bioimaging Potential of Fruit-Based Carbon Dots. *Nanomaterials* **2019**, *9*, 199, doi:10.3390/nano9020199.

40. Sendão, R.; Yuso, M. del V.M. de; Algarra, M.; Esteves da Silva, J.C.G.; Pinto da Silva, L. Comparative life cycle assessment of bottom-up synthesis routes for carbon dots derived from citric acid and urea. *J. Clean. Prod.* **2020**, *254*, doi:10.1016/j.jclepro.2020.120080.

41. Zhu, S.; Song, Y.; Zhao, X.; Shao, J.; Zhang, J.; Yang, B. The photoluminescence mechanism in carbon dots (graphene quantum dots, carbon nanodots, and polymer dots): current state and future perspective. *Nano Res.* 2015, *8*, 355–381.

42. Giovanella, U.; Pasini, M.; Botta, C. Organic Light-Emitting Diodes (OLEDs): Working Principles and Device Technology. In; Springer, Cham, 2016; pp. 145–196.

43. Squeo, B.M.; Pasini, M. BODIPY platform: a tunable tool for green to NIR OLEDs. *Supramol. Chem.* **2020**, *32*, 56–70, doi:10.1080/10610278.2019.1691727.

44. De Medeiros, T. V.; Manioudakis, J.; Noun, F.; Macairan, J.R.; Victoria, F.; Naccache, R. Microwave-assisted synthesis of carbon dots and their applications. *J. Mater. Chem. C* **2019**, *7*, 7175–7195, doi:10.1039/c9tc01640f.

45. Huang, C.C.; Hung, Y.S.; Weng, Y.M.; Chen, W.; Lai, Y.S. Sustainable development of carbon nanodots technology: Natural products as a carbon source and applications to food safety. *Trends Food Sci. Technol.* **2019**, *86*, 144–152, doi:10.1016/j.tifs.2019.02.016.

46. Ludmerczki, R.; Mura, S.; Carbonaro, C.M.; Mandity, I.M.; Carraro, M.; Senes, N.; Garroni, S.; Granozzi, G.; Calvillo, L.; Marras, S.; et al. Carbon Dots from Citric Acid and its Intermediates Formed by Thermal Decomposition. *Chem. – A Eur. J.* **2019**, *25*, 11963–11974, doi:10.1002/chem.201902497.

47. Yuan, F.; Li, S.; Fan, Z.; Meng, X.; Fan, L.; Yang, S. Shining carbon dots: Synthesis and biomedical and optoelectronic applications. *Nano Today* **2016**, *11*, doi:10.1016/j.nantod.2016.08.006.

48. Li, X.; Zhang, S.; Kulinich, S.A.; Liu, Y.; Zeng, H. Engineering surface states of carbon dots to achieve controllable luminescence for solid-luminescent composites and sensitive Be2+ detection. *Sci. Rep.* **2014**, *4*, 1–8, doi:10.1038/srep04976.

49. Kandasamy, G. Recent Advancements in Doped/Co-Doped Carbon Quantum Dots for Multi-Potential Applications. *C* **2019**, *5*, 24, doi:10.3390/c5020024.

50. Mandal, B.; Sarkar, S.; Sarkar, P. Exploring the electronic structure of graphene quantum dots. *J. Nanoparticle Res.* **2012**, *14*, doi:10.1007/s11051-012-1317-3.

51. Li, Y.; Shu, H.; Niu, X.; Wang, J. Electronic and Optical Properties of Edge-Functionalized Graphene Quantum Dots and the Underlying Mechanism. *J. Phys. Chem. C* **2015**, *119*, 24950–24957, doi:10.1021/acs.jpcc.5b05935.

52. Yamijala, S.S.; Bandyopadhyay, A.; Pati, S.K. Structural stability, electronic, magnetic, and optical properties of rectangular graphene and boron nitride quantum dots: Effects of size, substitution, and electric field. *J. Phys. Chem. C* **2013**, *117*, 23295–23304, doi:10.1021/jp406344z.

53. Güttinger, J.; Stampfer, C.; Frey, T.; Ihn, T.; Ensslin, K. Graphene quantum dots in perpendicular magnetic fields. *Phys. status solidi* **2009**, *246*, 2553–2557, doi:10.1002/pssb.200982312.

54. Li, X.; Lau, S.P.; Tang, L.; Ji, R.; Yang, P. Sulphur doping: A facile approach to tune the electronic structure and optical properties of graphene quantum dots. *Nanoscale* **2014**, *6*, 5323–5328, doi:10.1039/c4nr00693c.

55. Tao, S.; Zhu, S.; Feng, T.; Xia, C.; Song, Y.; Yang, B. The polymeric characteristics and photoluminescence mechanism in polymer carbon dots: A review. *Mater. Today Chem.* **2017**, *6*, doi:10.1016/j.mtchem.2017.09.001.

56. Guo, W.; Luo, Y.; Wei, K.; Gao, X. A cellular level biocompatibility and biosafety evaluation of mesoporous SiO2-based nanocomposite with lanthanum species. *J. Mater. Sci.* **2011**, *47*, 1514–1521, doi:10.1007/s10853-011-5938-1.

57. Ge, J.; Lan, M.; Zhou, B.; Liu, W.; Guo, L.; Wang, H.; Jia, Q.; Niu, G.; Huang, X.; Zhou, H.; et al. A graphene quantum dot photodynamic therapy agent with high singlet oxygen generation. *Nat. Commun.* **2014**, *5*, 1–8, doi:10.1038/ncomms5596.

58. Tang, L.; Ji, R.; Li, X.; Bai, G.; Liu, C.P.; Hao, J.; Lin, J.; Jiang, H.; Teng, K.S.; Yang, Z.; et al. Deep ultraviolet to near-infrared emission and photoresponse in layered n-doped graphene quantum dots. *ACS Nano* **2014**, *8*, 6312–6320, doi:10.1021/nn501796r.

59. Shamsipur, M.; Barati, A.; Karami, S. Long-wavelength, multicolor, and white-light emitting carbon-based dots: Achievements made, challenges remaining, and applications. *Carbon N. Y.* **2017**, *124*, doi:10.1016/j.carbon.2017.08.072.

60. Wang, Y.; Li, Y.; Yan, Y.; Xu, J.; Guan, B.; Wang, Q.; Li, J.; Yu, J. Luminescent carbon dots in a new magnesium aluminophosphate zeolite. *Chem. Commun.* **2013**, *49*, 9006–9008, doi:10.1039/c3cc43375g.

61. Song, Y.; Zhu, S.; Zhang, S.; Fu, Y.; Wang, L.; Zhao, X.; Yang, B. Investigation from chemical structure to photoluminescent mechanism: a type of carbon dots from the pyrolysis of citric acid and an amine. *J. Mater. Chem. C* **2015**, *3*, 5976–5984, doi:10.1039/C5TC00813A.

62. Xu, Q.; Kuang, T.; Liu, Y.; Cai, L.; Peng, X.; Sreenivasan Sreeprasad, T.; Zhao, P.; Yu, Z.; Li, N. Heteroatom-doped carbon dots: synthesis, characterization, properties, photoluminescence mechanism and biological applications. *J. Mater. Chem. B* 2016, *4*, 7204–7219.

63. Li, L.; Dong, T. Photoluminescence tuning in carbon dots: Surface passivation or/and functionalization, heteroatom doping. *J. Mater. Chem. C* **2018**, *6*, 7944–7970, doi:10.1039/c7tc05878k.

64. Yan, F.; Sun, Z.; Zhang, H.; Sun, X.; Jiang, Y.; Bai, Z. The fluorescence mechanism of carbon dots, and methods for tuning their emission color: a review. *Microchim. Acta* 2019, *186*.

65. Yuan, F.; Wang, Z.; Li, X.; Li, Y.; Tan, Z.; Fan, L.; Yang, S. Bright Multicolor Bandgap Fluorescent Carbon Quantum Dots for Electroluminescent Light-Emitting Diodes. *Adv. Mater.* **2017**, *29*, doi:10.1002/adma.201604436.

66. Ding, Y.; Zhang, F.; Xu, J.; Miao, Y.; Yang, Y.; Liu, X.; Xu, B. Synthesis of short-chain passivated carbon quantum dots as the light emitting layer towards electroluminescence. *RSC Adv.* **2017**, *7*, 28754–28762, doi:10.1039/c7ra02421e.

67. Miao, X.; Qu, D.; Yang, D.; Nie, B.; Zhao, Y.; Fan, H.; Sun, Z. Synthesis of Carbon Dots with Multiple Color Emission by Controlled Graphitization and Surface Functionalization. *Adv. Mater.* **2018**, *30*, doi:10.1002/adma.201704740.

68. Shi, L.; Yang, J.H.; Zeng, H.B.; Chen, Y.M.; Yang, S.C.; Wu, C.; Zeng, H.; Yoshihito, O.; Zhang, Q. Carbon dots with high fluorescence quantum yield: The fluorescence originates from organic fluorophores. *Nanoscale* **2016**, *8*, 14374–14378, doi:10.1039/c6nr00451b.

69. Song, Y.; Zhu, S.; Yang, B. Bioimaging based on fluorescent carbon dots. *RSC Adv.* 2014, *4*, 27184–27200.

70. Wang, L.; Li, W.; Yin, L.; Liu, Y.; Guo, H.; Lai, J.; Han, Y.; Li, G.; Li, M.; Zhang, J.; et al. Full-color fluorescent carbon quantum dots. *Sci. Adv.* **2020**, *6*, eabb6772, doi:10.1126/sciadv.abb6772.

71. Zheng, X.; Wang, H.; Gong, Q.; Zhang, L.; Cui, G.; Li, Q.; Chen, L.; Wu, F.; Wang, S. Highly luminescent

carbon nanoparticles as yellow emission conversion phosphors. *Mater. Lett.* **2015**, *143*, doi:10.1016/j.matlet.2014.12.138.

72. Joseph, J.; Anappara, A.A. White-Light-Emitting Carbon Dots Prepared by the Electrochemical Exfoliation of Graphite. *ChemPhysChem* **2017**, *18*, 292–298, doi:10.1002/cphc.201601020.

73. Wang, F.; Chen, Y.; Liu, C.; Ma, D. White light-emitting devices based on carbon dots' electroluminescence. *Chem. Commun.* **2011**, *47*, 3502, doi:10.1039/c0cc05391k.

74. Paulo-Mirasol, S.; Martínez-Ferrero, E.; Palomares, E. Direct white light emission from carbon nanodots (C-dots) in solution processed light emitting diodes. *Nanoscale* **2019**, *11*, 11315–11321, doi:10.1039/c9nr02268f.

75. Zhang, X.; Zhang, Y.; Wang, Y.; Kalytchuk, S.; Kershaw, S. V.; Wang, Y.; Wang, P.; Zhang, T.; Zhao, Y.; Zhang, H.; et al. Color-switchable electroluminescence of carbon dot light-emitting diodes. *ACS Nano* **2013**, *7*, 11234–11241, doi:10.1021/nn405017q.

76. Cappelli, A.; Villafiorita-Monteleone, F.; Grisci, G.; Paolino, M.; Razzano, V.; Fabio, G.; Giuliani, G.; Donati, A.; Mendichi, R.; Boccia, A.C.; et al. Highly emissive supramolecular assemblies based on π-stacked polybenzofulvene hosts and a benzothiadiazole guest. *J. Mater. Chem. C* **2014**, *2*, 7897–7905, doi:10.1039/c4tc01200c.

77. Botta, C.; Betti, P.; Pasini, M. Organic nanostructured host-guest materials for luminescent solar concentrators. *J. Mater. Chem. A* **2013**, *1*, 510–514, doi:10.1039/c2ta00632d.

78. Xu, J.; Miao, Y.; Zheng, J.; Wang, H.; Yang, Y.; Liu, X. Carbon dot-based white and yellow electroluminescent light emitting diodes with a record-breaking brightness. *Nanoscale* **2018**, *10*, 11211–11221, doi:10.1039/c8nr01834k.

79. Yuan, F.; Wang, Y.-K.; Sharma, G.; Dong, Y.; Zheng, X.; Li, P.; Johnston, A.; Bappi, G.; Fan, J.Z.; Kung, H.; et al. Bright high-colour-purity deep-blue carbon dot light-emitting diodes via efficient edge amination. *Nat. Photonics* **2020**, *14*, doi:10.1038/s41566-019-0557-5.

80. Jia, H.; Wang, Z.; Yuan, T.; Yuan, F.; Li, X.; Li, Y.; Tan, Z.; Fan, L.; Yang, S. Electroluminescent Warm White Light-Emitting Diodes Based on Passivation Enabled Bright Red Bandgap Emission Carbon Quantum Dots. *Adv. Sci.* **2019**, *6*, 1900397, doi:10.1002/advs.201900397.

81. Yuan, F.; Yuan, T.; Sui, L.; Wang, Z.; Xi, Z.; Li, Y.; Li, X.; Fan, L.; Tan, Z.; Chen, A.; et al. Engineering triangular carbon quantum dots with unprecedented narrow bandwidth emission for multicolored LEDs. *Nat. Commun.* **2018**, *9*, doi:10.1038/s41467-018-04635-5.

82. Singh, A.; Wolff, A.; Yambem, S.D.; Esmaeili, M.; Riches, J.D.; Shahbazi, M.; Feron, K.; Eftekhari, E.; Ostrikov, K. (Ken); Li, Q.; et al. Biowaste-Derived, Self-Organized Arrays of High-Performance 2D Carbon Emitters for Organic Light-Emitting Diodes. *Adv. Mater.* **2020**, *32*, 1906176, doi:10.1002/adma.201906176.

83. Xu, J.; Miao, Y.; Zheng, J.; Yang, Y.; Liu, X. Ultrahigh Brightness Carbon Dot–Based Blue

Electroluminescent LEDs by Host–Guest Energy Transfer Emission Mechanism. *Adv. Opt. Mater.* **2018**, *6*, 1800181, doi:10.1002/adom.201800181.

84. Park, Y.R.; Jeong, H.Y.; Seo, Y.S.; Choi, W.K.; Hong, Y.J. Quantum-Dot Light-Emitting Diodes with Nitrogen-Doped Carbon Nanodot Hole Transport and Electronic Energy Transfer Layer. *Sci. Rep.* **2017**, *7*, 1–13, doi:10.1038/srep46422.

85. Giovanella, U.; Pasini, M.; Lorenzon, M.; Galeotti, F.; Lucchi, C.; Meinardi, F.; Luzzati, S.; Dubertret, B.; Brovelli, S. Efficient Solution-Processed Nanoplatelet-Based Light-Emitting Diodes with High Operational Stability in Air. *Nano Lett.* **2018**, *18*, 3441–3448, doi:10.1021/acs.nanolett.8b00456.

86. Castelli, A.; Meinardi, F.; Pasini, M.; Galeotti, F.; Pinchetti, V.; Lorenzon, M.; Manna, L.; Moreels, I.; Giovanella, U.; Brovelli, S. High-Efficiency All-Solution-Processed Light-Emitting Diodes Based on Anisotropic Colloidal Heterostructures with Polar Polymer Injecting Layers. *Nano Lett.* **2015**, *15*, 5455–5464, doi:10.1021/acs.nanolett.5b01849.

87. Pasini, M.; Giovanella, U.; Betti, P.; Bolognesi, A.; Botta, C.; Destri, S.; Porzio, W.; Vercelli, B.; Zotti, G. The Role of Triphenylamine in the Stabilization of Highly Efficient Polyfluorene-Based OLEDs: A Model Oligomers Study. *ChemPhysChem* **2009**, *10*, 2143–2149, doi:10.1002/cphc.200900260.

88. Paulo-Mirasol, S.; Gené-Marimon, S.; Martínez-Ferrero, E.; Palomares, E. Inverted Hybrid Light-Emitting Diodes Using Carbon Dots as Selective Contacts: The Effect of Surface Ligands. *ACS Appl. Electron. Mater.* **2020**, *2*, 1388–1394, doi:10.1021/acsaelm.0c00163.

89. Alam, M.B.; Yadav, K.; Shukla, D.; Srivastava, R.; Lahiri, J.; Parmar, A.S. Carbon Quantum Dot as Electron Transporting Layer in Organic Light Emitting Diode. *ChemistrySelect* **2019**, *4*, 7450–7454, doi:10.1002/slct.201901551.

90. Zhang, X.; Zeng, Q.; Xiong, Y.; Ji, T.; Wang, C.; Shen, X.; Lu, M.; Wang, H.; Wen, S.; Zhang, Y.; et al. Energy Level Modification with Carbon Dot Interlayers Enables Efficient Perovskite Solar Cells and Quantum Dot Based Light-Emitting Diodes. *Adv. Funct. Mater.* **2020**, *30*, 1910530, doi:10.1002/adfm.201910530.

91. Circular-Consumer-Electronics-2704.